INSTITUT PASTEUR

ELSEVIER

Microbes and Infection 9 (2007) 1581–1589

www.elsevier.com/locate/micinf

Original article

Integration of HIV-1 caused STAT3-associated B cell lymphoma in an AIDS patient

Harutaka Katano [a,*], Yuko Sato [a], Satomi Hoshino [b], Natsuo Tachikawa [c], Shinichi Oka [c], Yasuyuki Morishita [d], Takaomi Ishida [e], Toshiki Watanabe [e], William N. Rom [b], Shigeo Mori [f], Tetsutaro Sata [a], Michael D. Weiden [b], Yoshihiko Hoshino [b,**]

[a] *Department of Pathology, National Institute of Infectious Diseases, 1-23-1 Toyama, Shinjuku, Tokyo 162-8640, Japan*
[b] *Division of Pulmonary and Critical Care Medicine, Department of Medicine, New York University School of Medicine, New York, NY 10016, USA*
[c] *AIDS Clinical Center, International Medical Center of Japan, Tokyo 162-8655, Japan*
[d] *Department of Pathology, Graduate School of Medicine, University of Tokyo, Tokyo 113-0033, Japan*
[e] *Department of Medical Genome Sciences, Graduate School of Frontier Sciences, University of Tokyo, Tokyo 108-8639, Japan*
[f] *Department of Pathology, Teikyo University School of Medicine, Tokyo 173-8605, Japan*

Received 26 June 2007; accepted 4 September 2007
Available online 14 September 2007

Abstract

Signal transducer and activator of transcription 3 (STAT3) is a DNA-binding transcription factor activated by multiple cytokines and interferons. High expression of STAT3 has also been implicated in cancer and lymphoma. Here, we show a case of B cell lymphoma in which a defective human immunodeficiency virus 1 (HIV-1) integrated upstream of the first STAT3 coding exon. The lymphoma cells with anaplastic large cell morphology formed multiple nodular lesions in the lung of an acquired immunodeficiency syndrome (AIDS) patient with Kaposi's sarcoma. The provirus had a 5′ long terminal repeat (LTR) deletion, but the 3′ LTR had stronger promoter activity than the STAT3 promoter in reporter assays. Immunohistochemistry showed increased expression of STAT3 in the nuclei of lymphoma cells. Transfection of STAT3 resulted in transient cell proliferation in primary B cells in vitro. Although this is a very rare case of HIV-1-integrated lymphoma, these data suggest that up-regulation of STAT3 caused by HIV-1 integration resulted in the development of B cell lymphoma in this special case.

Keywords: HIV-1; Integration; AIDS-related lymphoma; STAT3

1. Introduction

Malignant lymphoma is an important complication of patients with acquired immunodeficiency syndrome (AIDS). A large part of AIDS-related lymphomas are of B cell linage, and positive for Epstein–Barr virus (EBV) or Kaposi's sarcoma-associated herpesvirus (KSHV) [1–4]. Since human immunodeficiency virus 1 (HIV-1) is not usually detected in AIDS-related lymphoma cells, HIV-1 infection plays an indirect role in lymphomagenesis by impairing host immune surveillance. However, proviral DNA can either disrupt expression of tumor suppressor genes or enhance expression of cellular oncogenes. Alternatively, retroviral promoters can integrate into the host genome in such a manner that expression of a nearby oncogene is enhanced by a strong promoter within the proviral 3′-long terminal repeat (3′LTR). In humans, abnormal T cell proliferation following gene therapy for severe combined immunodeficiency resulted from retroviral integration into the intron of the *LMO2* proto-oncogene [5].

* Corresponding author. Tel.: +81 3 5285 1111; fax: +81 3 5285 1189.
** Corresponding author. Departments of Environmental Medicine and Medicine, New York University School of Medicine, 462 First Avenue NB 8E38, New York, NY 10016, USA. Tel.: +1 212 263 7770; fax: +1 212 263 8501.
E-mail addresses: katano@nih.go.jp (H. Katano), hoshiy01@gcrc.med.nyu.edu (Y. Hoshino).

1286-4579/$ - see front matter © 2007 Elsevier Masson SAS. All rights reserved.
doi:10.1016/j.micinf.2007.09.008

In AIDS patients, some cases of lymphomas had HIV-1 integration within the *fur* gene, just upstream from the *c-fes/fps* proto-oncogene [6]. That report, however, did not investigate the functional effect of this integration event. These observations suggest that HIV-1 may contribute directly to lymphomagenesis by inserting an active promoter into a cellular oncogene [6]. In the present study, we report a case of AIDS-related lymphoma in which HIV-1 integrated upstream of the STAT3 gene. The association of HIV-integration and lymphomagenesis was investigated.

2. Materials and methods

2.1. Samples

Lymphoma tissues in the lung of a patient with HIV-1 infection were obtained at autopsy. Formalin-fixed pathological samples of lymphoma, including nine unrelated cases of AIDS-related lymphoma and 15 cases of non-Hodgkin lymphoma in HIV-1-uninfected individuals, were studied. All samples were obtained with informed consent according to the Declaration of Helsinki. The study protocol was approved by the institutional review board of National Institute of Infectious Diseases (Approval No. 93).

2.2. Immunohistochemistry and in situ hybridization

Immunohistochemistry was performed as described before [7,8]. Primary antibodies were: anti-CD3 (Dako, Copenhagen, Denmark), CD20 (Dako), CD30 (Dako), CD45 (Dako), CD45RO (Dako), CD79a (Dako), CD138 (Serotec, Oxford, UK), and $p80^{NPM/ALK}$ (Nichirei, Tokyo, Japan), STAT3 (sc8019, Santa Cruz Biotechnology, Santa Cruz, CA), pSTAT3 (sc8059, Santa Cruz), KSHV-encoded LANA [8], and vIL-6 [7] antibodies. In situ hybridization for EBERs was performed as described before [9].

2.3. PCR and DNA sequences

PCR detection for KSHV-encoded open reading frame (ORF) 26, EBV W region, HIV-1 V3, and β-globin gene was performed as described previously [9,10]. For PCR amplification of HIV-1 3′LTR and STAT3 junction, HIV3LTR-F (5′-TCTGAGCCTGGGAGCTCTCT-3′, 9561–9580 in GenBank K03455) and Stat3intron-R (5′-AGTGCATGGCACATAACAGA-3′, 41131–41150 in GenBank AY572796) were used. For amplification of HIV-1 5′LTR and STAT3 junction, 6 reverse primers of 5′LTR (55R 5′-TCAGGGAAGTAGCCTTGTGTGTGGT-3′, 78R 5′-GCCCTGGTGTGTAGTTCTGTCAATC-3′, 348R 5′-GAAAGTCCCCAGTGGAAAGTCCCTT-3′, 495R 5′-GCAGTGGGTTCCCTAGTTAGCC-3′, 563R 5′-TTACCAGAGTCACACAACAGACGGG-3′, and 612R 5′-CACTGCTAGAGATTTTCCACACTGAC-3′), and a reverse primer positioning between 5′LTR and gag (676R 5′-CGAGTCCTGCGTCGAGAGATCTCCT-3′) were used with a forward primer of Stat3-intronF2 (5′-CATTTTTCTTTCCTTCTCTGTTGTC-3′, 40881–40905 in GenBank AY572796). These primers for HIV-1 were designed based on the sequence of HIV-1 IIIB (GenBank K03455).

2.4. Cloning of HIV-1 integration sites

The methods used were essentially as described for the Gene Walker Kit (BD Clontech, Palo Alto, CA). Lung tumor DNA was cleaved with four different blunt cutting enzymes (*Dra*I, *Eco*RV, *Pvu*II and *Ssp*I). Gene specific primers for HIV-1 LTR were 5′-ACCACACACAAGGCTACTTCCCTGA-3′ (GSP-1) and 5′-AAGGGACTTTCCACTGGGGACTTTC-3′ (GSP-2).

2.5. Real-time PCR

Copy numbers of HIV-1 integration site and STAT3 gene were measured with real time PCR as described previously [11]. Two probe and primer sets were used (Set 1: forward primer: 5′-CTAGAGATCCCTCAGACCATTTTAGTC-3′, reverse: 5′-AAAAGTATAAATGAGGATCCAGGAAGAT-3′, probe: 5′-6FAM-TGTGGAAAATCTCTAGCAGAATCTCAGG-TAMRA-3′; Set 2: forward primer: 5′-GCAGCTTGACACACGGTACCT-3′, reverse: 5′-AAACTGCCGCAGCTCCATT-3′, probe: 5′-6FAM-AGCAGCTCCATCAGCTCTACAGTGACAGC-TAMRA-3′).

2.6. Plasmids

For the promoter assay, genes of the HIV-1 3′LTR, STAT3-intron (40951–41959 of GenBank AY572796), and STAT3-promoter (1–1998 of GenBank AY572796) were amplified from DNA of the HIV-1-integrated lymphoma using the LTR-*Mlu*I-F, 5′-GAG*ACGCGT*TGGAAGGGCTAATTCACTCCC-3′ and LTR-*Xho*I-R, 5′-GTG*CTCGAG*TGCTAGAGATTTTCCACACT-3′, the Intron-*Mlu*I-F, 5′-GAG*ACGCGT*GAATCTCAGGCAGATCTTCC-3′ and Intron-*Xho*I-R, 5′-CAC*CTCGAG*CCTGCTAAAATCAGGGGTCCC-3′, and, the Stat3prom-*Mlu*F1, 5′-GAG*ACGCGT*ACCCATAGTCGCAGAGGTAGA-3′ and Stat3prom-*Xho*R1, 5′-GAG*CTCGAGCGCTGAATTACAGCCCCTTCA-3′, respectively. Enzyme sites are indicated in italics. A fragment of the HIV-1 3′LTR was amplified also from HIV-1 pNL4-3 (GenBank AF324493). The PCR product was subcloned into *Mlu*I-*Xho*I site of pGL3-basic vector (Promega, Madison, WI). For the STAT3-expression plasmid, STAT3 cDNA was amplified from the mammalian gene collection-human (MGC-1607, American type culture collection, Manassas, VA) using forward primer (STAT3-HpaI-F10 5′-CACCGTTAACGGATCCTGGACAGGCACCC-3′) and reverse primer (STAT3-R24 5′-CATGTCAAAGGTGAGGGACTCAAA-3′). The PCR product was TA cloned using pcDNA 3.1 Directional TOPO Expression kit (Invitrogen, Carlsbad, CA). For cell proliferation experiment, the STAT3 expression vector was digested with *Hin*dIII and *Eco*RV and ligated into *Bsm*BI and *Eco*RV sites of pMACS 4-IRES.II vector, which is a bicistronic expression vector containing multiple cloning site followed by an internal ribosome entry site (IRES) element

from encephalomyocarditis virus and the truncated (non-functional) CD4 cDNA (Miltenyl Biotec, Auburn CA).

2.7. Promoter assay

Plasmids were transiently transfected into HeLa cells with a renilla reporter gene construct using Lipofectamine Plus (Invitrogen). Luciferase activity was measured with a dual luciferase assay system (Promega). In the HIV-1-Tat (+) group, an HIV-1-Tat expression vector, kindly provided by Dr. Kenzo Tokunaga, National Institute of Infectious Diseases, Tokyo, Japan, was cotransfected.

2.8. DNA methylation analysis

Methylation of the cytosine residue of the CpG site was analyzed by the bisulfite genomic sequencing method, as described previously [12]. The primer pair for selective analysis was as follows: sense primer, 5′-TATAAACCAGCATGG GATGGATGA-3′; antisense primer, 5′-CCCAGGCTCGGA TCTGGTCTAACC-3′.

2.9. Cell proliferation assay for primary lymphocytes

Primary B cells were negatively selected from whole blood of healthy volunteers using RosetteSep B cell enrichment (StemCell Technology, Vancouver, BC, Canada) [13]. Cell proliferation assay was performed using BrdU Cell proliferation ELISA kit (Roche Molecular Biochemicals, Indianapolis, IN).

3. Results

3.1. HIV-1 was concentrated in lymphoma cells in a case of AIDS-related lymphoma

A 59-year-old, homosexual, HIV-1-positive male with a CD4 cell count of 6/mm^3 showed high fever and multiple KS skin lesions. Computed tomography scanning revealed multiple nodules in the lung (Fig. 1A). Despite treatments with antibiotics and combined chemotherapy, with intensive care, he died 30 days after admission. The clinical course of the patient was also reported previously [14]. At autopsy, multiple nodules were present in the lung (Fig. 1B). Histologically, these nodules were composed of large atypical cells with anaplastic large cell morphology infiltrating into interstitial and alveolar areas in the lung tissue (Fig. 1C). Immunohistochemistry demonstrated that the tumor cells were CD3$^-$, CD20$^-$, CD30$^+$, CD45$^+$, CD45RO$^+$, CD79a$^-$, CD138$^-$, and p80$^{NPM/ALK-}$, suggesting that the lung tumor was composed of lymphoma cells (Fig. 1D and data not shown) [14]. Southern blot hybridization of DNA extracted from the lung tumor with an immunoglobulin junction hinge (JH) probe demonstrated immunoglobulin gene rearrangement, confirming a B

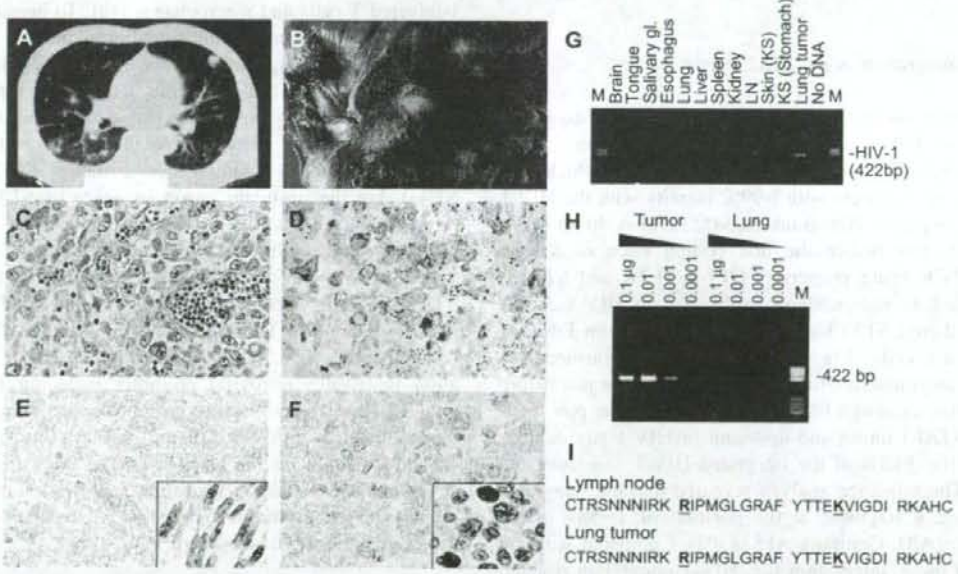

Fig. 1. Pathological findings of tumors in the lung of a patient with AIDS. CT scan (A), macroscopic view (B) and Hematoxylin and eosin staining (C) of the lung tumor. (D) Immunohistochemistry of CD45RO. (E) Immunohistochemistry for KSHV-LANA in the lung tumor cells. Inset shows gastric KS cells from the patient. (F) In situ hybridization for EBV-EBER in the lung tumor cells. Inset shows a positive control of EBV-positive lymphoma from an unrelated patient. (G) PCR detection for HIV-1 V3 region in various organs of the patient. LN, lymph node; M, DNA molecular weight marker (pBR322/*Hae*III). (H) Semi-quantitative PCR for HIV-1. DNA quantities are indicated at the top of the panel. DNA extracted from the lung tumor and surrounding lung tissues was tested. (I) Predicted amino acid sequence of HIV-1 gp120 V3 loop of HIV-1 amplified from the lymph node and lung tumor by PCR. Positions 11 and 25 are indicated by bold letters with underlines. DNA sequences are deposited in GenBank under accession numbers DQ116951 to DQ116954 (HIV-1 envelope from LN and lung tumor).

cell linage (data not shown). Since KS lesions were found in the oral cavity, stomach, sole and some lymph nodes at autopsy, we examined KSHV positivity in the lymphoma (lung tumor). KSHV-encoded ORF26 was amplified in both gastric KS lesions and lung tumor by PCR (data not shown). However, immunohistochemistry demonstrated that expression of KSHV LANA was very weak or absent in the lymphoma cells, whereas KS cells in the stomach strongly expressed LANA (Fig. 1E). Immunohistochemistry also demonstrated that the lung tumor cells were negative for KSHV-encoded vIL-6 (data not shown). The lymphoma cells were positive for EBV by PCR (data not shown), but in situ hybridization failed to detect EBERs (Fig. 1F). Thus, these data suggest that KSHV and EBV were present in the lymphoma at low copy numbers. Surprisingly, HIV-1 DNA was detected in the lymphoma cells by PCR, but not in other organs besides the lymph nodes (Fig. 1G). Semi-quantitative PCR revealed that there was a 100-fold higher copy number of HIV-1 DNA from the lymphoma than from surrounding lung tissue (Fig. 1H). PCR products of HIV-1 V3 region were TA-cloned and each 10 clones were sequenced. Although two (clones L2 and T3) and three (clones T1, T3, and T6) kinds of sequences were obtained from the lymph nodes and lymphoma, respectively, all sequences coded the same amino acid sequence in the V3 loop (net charge = + 7). Basic amino acids at positions 11 and 25 of the gp120 V3 loop and a high positive net charge strongly suggest that fusogenic X4 viruses were detected in the lymphoma cells and lymph nodes (Fig. 1I) [15].

3.2. HIV-1 integration in the STAT3 gene

A high copy number of HIV-1 in the lymphoma suggested integration of HIV-1 into the genome of lymphoma cells. Genome walking PCR produced a 400 bp fragment which contained a 300 bp fragment with >99% identity with the HIV-1 IIIB 3′LTR sequence (GenBank K03455) and A 40 bp genomic segment just before the first coding exon of STAT3 (Fig. 2A). PCR using primers in HIV-1 3′LTR and STAT3-intron yielded an independent amplicon with HIV-1 3′LTR and the predicted STAT3 genomic sequences from DNA of the lymphoma cells (Fig. 2B). These data confirmed that HIV-1 had integrated into the intervening sequence just before the first coding exon of STAT3. PCR using a primer pair binding to the STAT3 intron and upstream of HIV-1 gag demonstrates that the 5′LTR of the integrated HIV-1 was truncated (Fig. 2C). The sequence analysis revealed that the integrated HIV-1 lacked a fragment at the position of 1–587 in the 5′LTR (Fig. 2A,D, GenBank AF538307). Compared with the sequence of the 3′ integration site, HIV-1 integration resulted in duplication of the cellular 5 bp (GAATC) and addition of a dinucleotide at the integration site by HIV-1 integrase, which is commonly seen among retrovirus integrases [16,17]. Consequently, the integration event was produced by a defective virus (Fig. 2A,D). The absence of p24-staining of the tumor is consistent with this conclusion (data not shown).

3.3. Copy number of the integrated HIV-1 in the lymphoma tissue

Generally, pathological tissues obtained from lymphoma lesions contain not only lymphoma cells, but also surrounding CD4-positive T cells or alveolar macrophages. Although immunohistochemistry demonstrated no or rare CD4-positive cells in the lymphoma tissue, we tried to determine a copy number of the integrated HIV-1 in the lymphoma tissue by a real time PCR targeting genes near the integration site to deny the possibility that HIV-1 integration was originated in the contaminated CD4-positive cells (Fig. 3). A fragment of HIV-1-integration site was amplified at 12,570 copies/100 ng of DNA by the real time PCR, whereas exon 1 of STAT3 gene was amplified at 121,597 copies/100 ng. Since each cell has two copies of STAT3 gene on two alleles, these data suggest that HIV-1 integration occurred about 20% of the population that the DNA was extracted from. As shown in Fig. 1C, the lymphoma tissue contained many cells other than lymphoma cells, such as alveolar epithelial cells, macrophages, and endothelial cells. However, CD4-positive T cells were rare in the tissue, and the HIV-1 was X4 virus. Therefore, these data suggest that the HIV-1 might be detected from lymphoma cells, not from contaminated T cells or macrophages, and integrate into more than 20% of the lymphoma cells.

3.4. Promoter activity and methylation of HIV-1 3′LTR

LTRs of HIV-1 usually have a promoter activity in HIV-1-infected T cells and macrophages [18]. To investigate if the HIV-1 3′LTR contained a functional promoter, we constructed a plasmid containing the patient's HIV-1 3′LTR or upstream intron sequence of STAT3 before a luciferase reporter gene. Transfection of the plasmid to HeLa cells revealed that the sequence of 3′LTR derived from the patient had significant promoter activity at a similar level to that of 3′LTR in HIV-1 NL4-3, but the upstream intron sequence of STAT3 did not (Fig. 4A). 3′LTR was a stronger promoter than the STAT3 promoter derived from the patient. Cotransfection with a plasmid expressing HIV-1-Tat enhanced the activity of the patient's 3′LTR 31-fold, whereas the activity of the STAT3 promoter was not enhanced. These data suggest that the HIV-1 3′LTR contains promoter activity. It is known that DNA CpG methylation inactivates retroviral promoter including HIV-1 LTR [12,19]. However, a bisulfite genomic sequence revealed that the fragment of HIV-1 3′LTR did not have any CpG or non-CpG methylation in the DNA extracted from the lymphoma (Fig. 4B,C). These data suggest that methylation might not reduce or inhibit the transcriptional activity of HIV-1 3′LTR in the HIV-1-integrated lymphoma cells.

3.5. Expression of STAT3 in the HIV-1-integrated lymphoma

We investigated expression of STAT3 in the case of HIV-1-integrated lymphoma. Immunohistochemistry demonstrated a high level of STAT3 expression predominantly in the nuclei

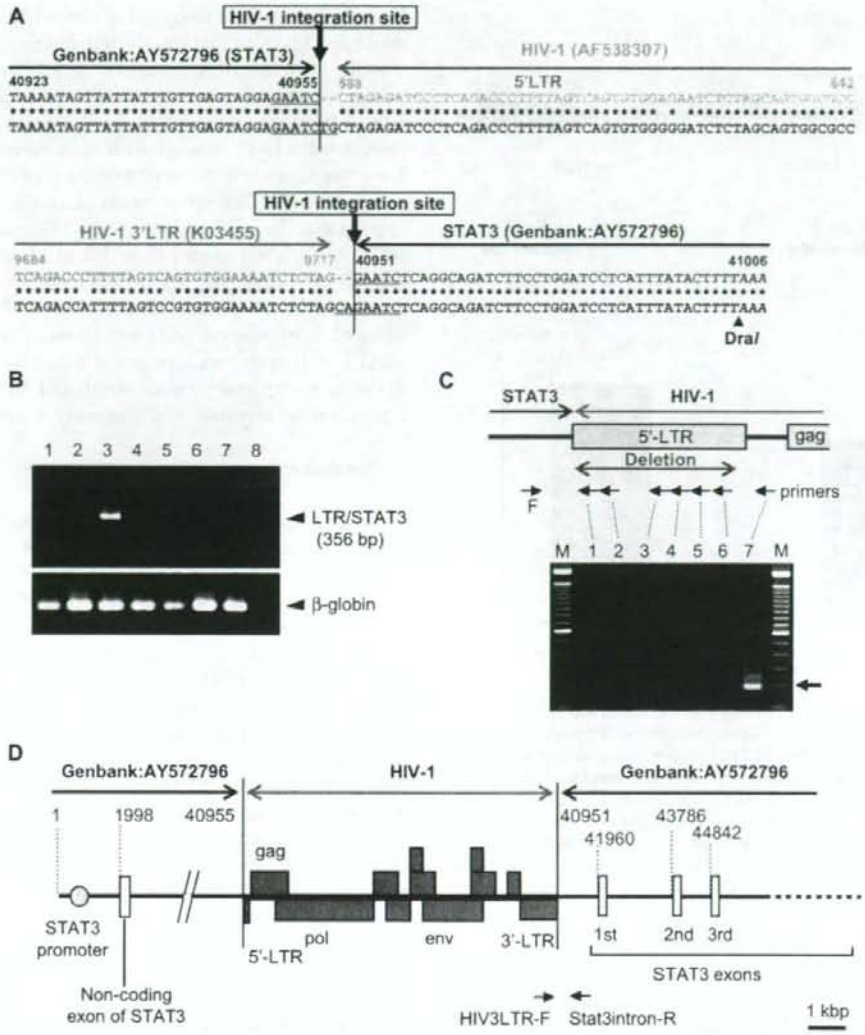

Fig. 2. Identification of HIV-1 integration site in the lymphoma cells with genome walking. (A) Sequence of the HIV-1 5′-LTR (upper panel) and 3′-LTR (lower panel) insertion site in the lymphoma genome. Whole sequences of PCR products are registered as GenBank DQ355432 (5′-LTR, 190 bp) and DQ117603 (3′-LTR, 1.5 kbp), respectively. The sequence of the lymphoma genome is shown in the lower line in black letters. The upper colored line indicates the HIV-1 LTR sequence (blue, GenBank K03455 or AF538307) and STAT3 genomic sequence (violet, GenBank AY572796). HIV-1 intervening sequence between 5′LTR and gag is indicated by green. Duplication of the cellular 5 bp (GAATC) and additional dinucleotides (TG in 5′-LTR and CA in 3′-LTR) by HIV-1 integrase are underlined. *DraI* site is indicated by italics. (B) PCR for the junction region of 3′LTR and STAT3 gene using HIV3LTR-F and Stat3intron-R primers (see Fig. 3D). 1, PBMCs from a healthy donor; 2, HIV-1-positive Molt4 cell line; 3, lymphoma cells with HIV-1integration; 4, KS lesion from the patient; 5, AIDS-related lymphoma from an unrelated patient; 6, lymphoma from a non-HIV-1infected patient; 7, BCBL-1 (KSHV-positive B cell line); 8, No DNA. The lower panel shows the results of an internal control (β-globin gene). (C) PCR of genomic DNA with a STAT3-intron forward primer (F in this figure, Stat3-intronF2) in combination with 5′ LTR reverse primers (lanes 1–6, 55R, 78R, 348R, 495R, 563R and 612R), and a reverse primer positioning between 5′LTR and gag (lane 7, 676R). The upper panel shows the positions of these primers. A 188 bp product was identified when the 676R primer was used with the STAT3 intron primer (lane 7). If the 5′LTR was intact, the predicted size of this amplicon would have been 777 bp. (D) Map of the defective HIV-1 insertion site in the STAT3 gene. Violet numbers indicate the number in GenBank AY572796 (STAT3). Blue boxes are HIV-1 genomes.

of the HIV-1-integrated lymphoma cells (Fig. 4D). To know the phosphorylation status of STAT3, we immunostained the slide using an anti-pSTAT3 (Tyr-705) antibody as a primary antibody. However, any signal was not found in the lymphoma cells (data not shown). We also examined STAT3 expression in 24 cases of lymphoma, including nine cases of AIDS-related lymphoma and 15 of non-AIDS-related lymphoma, normal tonsilar tissues and lymph nodes derived from unrelated patients. The nine cases of AIDS-related lymphoma contained seven of EBV-positive diffuse large B cell lymphoma

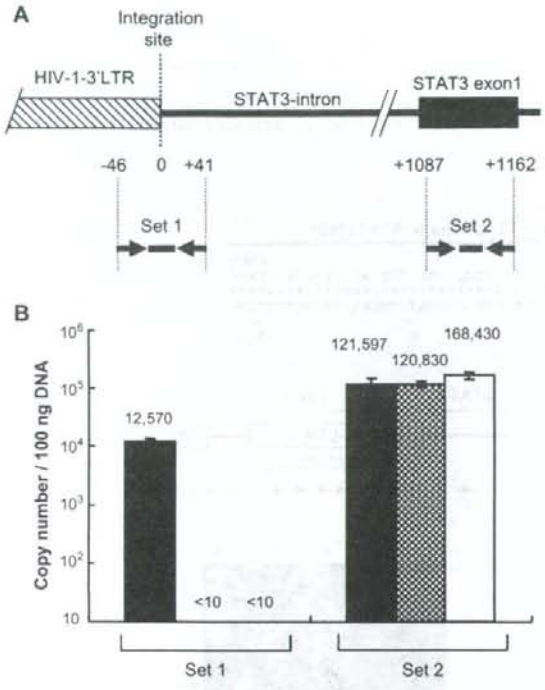

Fig. 3. Quantitative analysis of genes for HIV-1 integration site. (A) Probe-primer sets for real time PCR. The top line with boxes is a genome map around HIV-1 integration site of HIV-1 3'LTR. Numbers with plus and minus under the genome map indicate distances (bp) from the integration site. Arrows and heavy lines are probe-primer sets of real time PCR. (B) Copy numbers of HIV-1 integration site and STAT3 gene. Black, gray and white bars indicate mean copy number per 100 ng DNA of this case, HIV-1-positive Molt4 cell line, and TY-1 (HIV-1-negative, KSHV-positive B cell line), respectively. Copy numbers per 100 ng DNA are indicated on the top of each bar. Error bars indicate standard errors of triplicate samples.

(DLBCL), and two cases of Hodgkin's disease. The 15 cases of non-AIDS-related lymphoma contained 12 EBV-positive or EBV-negative DLBCL and three cases of Hodgkin's disease. Immunohistochemistry revealed that several cases of AIDS-related lymphoma and one of HIV-unrelated lymphoma expressed STAT3 predominantly in the cytoplasm (Fig. 4E); however, no case expressed STAT3 predominantly in the nucleus (Table 1). STAT3 expression was not found, or was weak, in other cases examined (Fig. 4F). These data suggest that the integration of HIV-1 induced high expression of STAT3 in the lymphoma cells of the patient.

3.6. Transfection of STAT3 expression plasmid to primary B cells in vitro

To investigate if expression of STAT3 induces cell growth, we constructed an expression plasmid for STAT3 and transfected the plasmid to B cells. At first, to confirm expression of STAT3 by Nucleofector transfection, His-tagged STAT3 was expressed in TY-1, a KSHV-positive B cell line. Immunofluorescence assay using anti-STAT3 and anti-6x His antibodies revealed that transfection efficiency to lymphocytes was 30–40% in this experiment (Fig. 5A). Addition of IL-6 to culture medium of transfected TY-1 altered the localization of STAT3 from the cytoplasm to the nucleus, suggesting that the transfected STAT3 reacted with IL-6 stimulation (Fig. 5B). Then, we investigated the proliferation of STAT3-transfected primary B cells. Cell proliferation assay after 48 h transfection showed that the proliferation of STAT3-transfected primary B cells were slightly higher than that of vector-transfected primary B cells (Fig. 5C, Mann–Whitney test, $p < 0.01$). However, 4 days after transfection, the difference was not statistically significant (data not shown). The transfection of STAT3 to B cells was repeated 4 times with similar results. These data suggested that transfection of STAT3 might induce a transient proliferation in the primary B cells in vitro.

4. Discussion

In the present study, we present a case of AIDS-related B cell lymphoma with HIV-1 integration. HIV-1 with defective 5'LTR integrated into the upstream region of the first STAT3 coding exon. The 3' LTR had strong promoter activity, resulting in increased expression of STAT3 in the nuclei of lymphoma cells. This is the first case report describing dysregulation of STAT3 by HIV-1 integration, resulting in B cell lymphoma development.

STAT3 is an important molecule for IL-6-type cytokines that signal and stimulate proliferation and terminal differentiation of B cells [20]. STAT3 also plays some oncogenic roles. Activated and phosphorylated STAT3 has been observed in a variety of experimental and numerous human malignancies [21–23]. A recent study reveals that high expression of unphosphorylated STAT3 results in up-regulation of oncogenes, suggesting that overexpression of either form of STAT3, phosphorylated and unphosphorylated, might induce cancer [24]. Although we failed to detect phosphorylated STAT3, high expression of STAT3 in the nucleus implies that activated STAT3 may bind to DNA and activate some genes constitutively. Alternatively, it implies that overexpression of unphosphorylated STAT3 in the nucleus might induce various oncogenes such as cdc2, cyclin B1 and mras [24]. However, our transfection study of STAT3 resulted in transient cell proliferation in the primary B cells (Fig. 5), suggesting that additional factors other than STAT3 expression might be required for complete transformation of primary B cells. HIV-1 integrated into *c-fes/fps* in other reported cases of AIDS-related lymphoma [6], and it has been demonstrated that *c-fes* activates STAT3 [25]. Thus, STAT3 may play some roles in the lymphomagenesis in the cases of HIV-1-integrated lymphoma.

This case was B cell lymphoma. HIV-1 usually infects and integrates into T cells or macrophages, and it is uncommon for HIV-1 to infect B cells. In the report by other group, HIV-1 provirus was frequently detected in macrophages infiltrating lymphomas, not in lymphoma cells [6]. However, in our case, we concluded that the HIV-1 integration occurred in the lymphoma cells, not in T cells or macrophages infiltrating

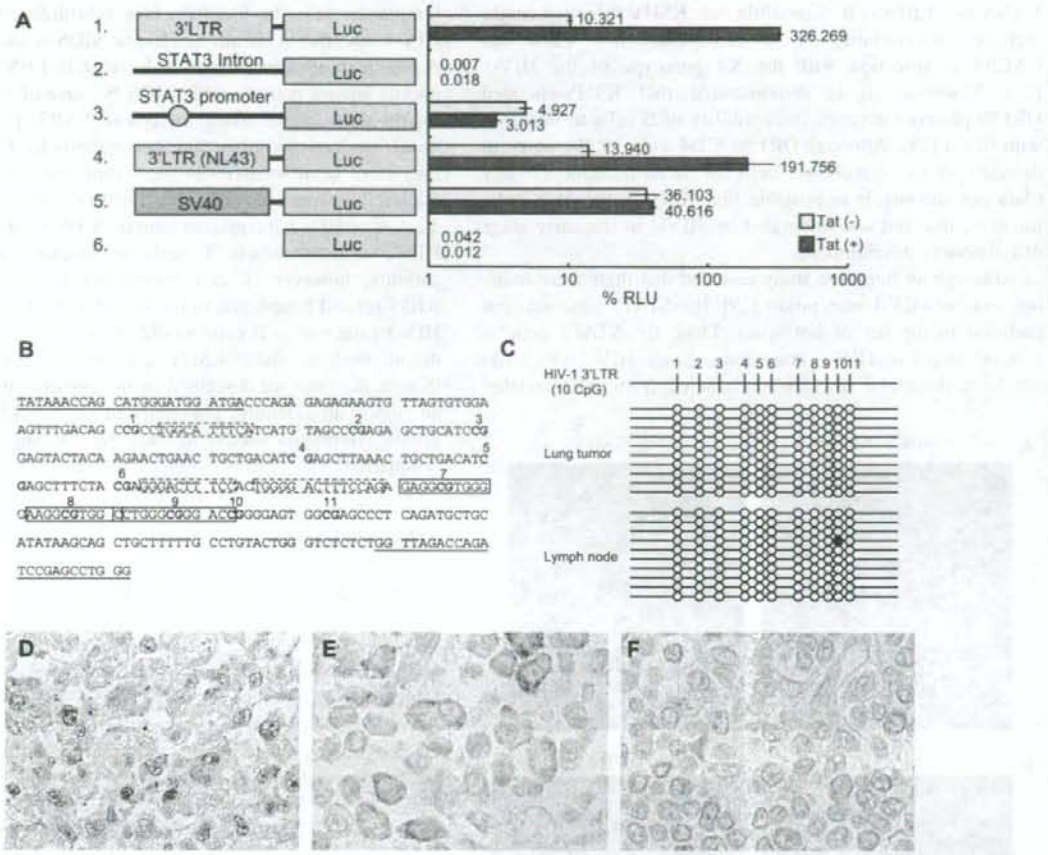

Fig. 4. Promoter activity of HIV-1 3′LTR and STAT3 expression in the lymphoma. (A) Promoter activity of HIV-1 3′LTR by reporter assay. Schematic representation of promoter constructs used in transient transfection assays is shown on the left. Forty-eight hours after transfection, cells were collected and the luciferase activity was measured. The percentage relative luminescence units (RLU) were calculated by dividing firefly activity by renilla activity. Horizontal bars indicate standard deviations of three independent experiments. (B and C) No methylation in a promoter enhancer region of HIV-1 3′LTR in the HIV-1-integrated lymphoma. (B) CpG sites in the promoter enhancer region of 3′LTR of the HIV-1 provirus in the patient with HIV-1-integrated lymphoma (218–529 in GenBank DQ117603). CpG sites are in boldface and numbered from the 5′ end of the LTR (1–11). Nuclear factor-κB and Sp1 sites identified with Motif Search (Kyoto University Bioinfomatics center, Kyoto, Japan, http://motif.genome.jp/) at a 75% cut-off value are indicated by boxes with broken and solid lines, respectively. Sequences used for primers are indicated by underlining. (C) Levels of CpG methylation of the promoter enhancer region of HIV-1 3′LTR in the HIV-1-integrated lymphoma and lymph nodes in the patient. Results of bisulfite genomic sequencing coupled with TA cloning are shown. The methylation status of 10 clones for each sample is presented; methylation of each CpG site is expressed as a filled circle, and unmethylated sites are shown as open circles. Top, schematic description of CpG sites in the 3′LTR of (B). (D–F) Immunohistochemistry of STAT3. The HIV-1-integrated lymphoma cells expressed STAT3 predominantly in the nucleus (D), however, signals of STAT3 were weak and localized in the cytoplasm in the other case of KSHV-positive, AIDS-related lymphoma (E), and were very weak in a case of EBV-positive, AIDS-related lymphoma (F). Original magnification is ×400.

in the lymphoma, because of following reasons: (1) there were few T cells in the lymphoma tissue by immunohistochemistry for CD3 (data not shown); (2) HIV-1 DNA was detected in the lymphoma at a high copy number, that is very rare or none in AIDS-related lymphoma [26]; (3) HIV-1 sequences suggested the possibility of X4 viruses, which leads the integrated HIV-1 sequences are usually not found in the macrophages; (4) some different HIV-1 V3 sequences were identified between the lymphoma and lymph node; and (5) the titer of HIV-1 DNA in the lymphoma were higher than that in the lymph node (Fig. 1G). Then, how did HIV-1 infect B cells in the patient? Although detail mechanism of HIV-1 infection to B cells in this case was still unknown, we presume that KSHV played an important role in HIV-1 infection to B cells. This case of lymphoma was positive for KSHV and EBV by PCR, however, KSHV and EBV did not play a direct role in the oncogenesis of the lymphoma because of the low or absent expression of

Table 1
STAT3 expression in AIDS-related and unrelated lymphoma

STAT3 expression	Nucleus	Cytoplasm	No expression	Total
AIDS-related lymphoma	1*	7	2	10
Non-AIDS-related lymphoma	0	1	14	15

*HIV-integrated lymphoma reported in the present study.

LANA and EBERs. It is possible that KSHV infection might increase susceptibility of B cells expressing CD4 and CXCR4 to infection with the X4 genotype of the HIV-1 [27]. Moreover, it is demonstrated that KSHV-encoded ORF50 protein increases susceptibility of B cells to infection with HIV-1 [28]. Although ORF50, CD4 and CXCR4 were not detected in the lymphoma cells by immunohistochemistry (data not shown), it is possible that KSHV-infected B cells might be infected and integrated by HIV-1 in the early stage of lymphoma development.

Although an intensive study revealed that there were many hot spots of HIV-1 integration [29], the STAT3 gene was not included in the list of hot spots. Thus, the STAT3 gene is a novel target of HIV-1 integration. Since HIV-1 DNA has not been detectable in DNAs extracted from AIDS-related lymphoma cases by Southern blot hybridization, so far [26], HIV-1 integration should be rare in AIDS-related lymphoma. A recent study demonstrates a decrease in EBV-positive lymphoma among patients with AIDS because of introduction of highly active antiretroviral therapy (HAART) [30]. Therefore, novel mechanisms other than oncogenesis by EBV or KSHV may have been involved in the lymphomagenesis of AIDS-related lymphoma recently. There is no report describing a frequency of HIV-1 integration among AIDS related lymphoma. HIV-1 usually infects T cells or macrophages in AIDS patients, however, T cell lymphoma is still rare among AIDS-related lymphoma in the HAART era [30]. In addition, HIV-1 infection to B cells would occur in a very special condition, such as under KSHV infection. Taken together, although the case we described in the present study contained an important scientific phenomenon on STAT3, HIV-1-integrated lymphoma should be very rare among AIDS-related lymphoma.

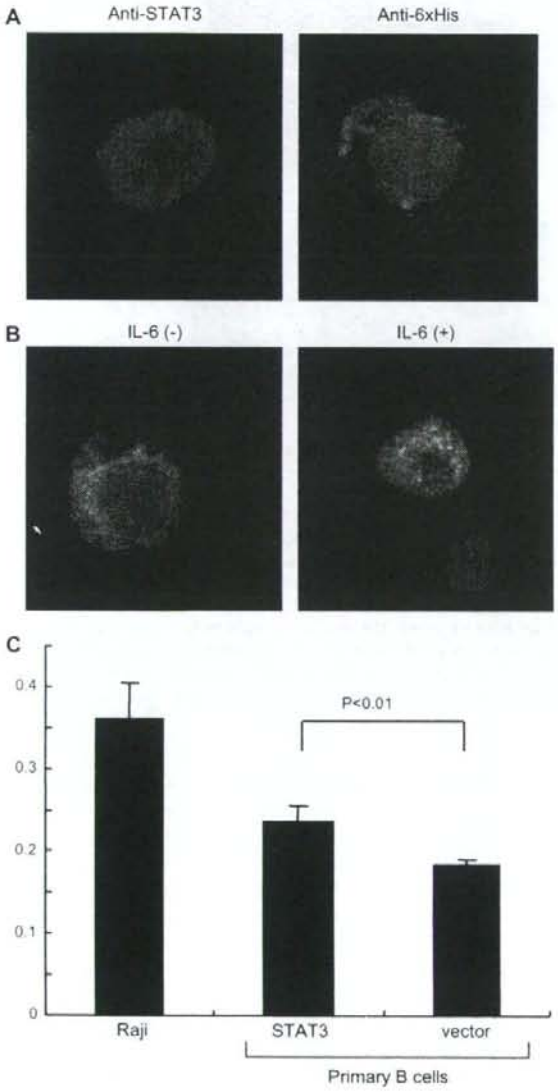

Fig. 5. Transfection of STAT3 into B cells in vitro. (A) STAT3 expression in the STAT3-transfected TY-1, a KSHV-positive B cell line. The cells were transfected with STAT3 expression vector by Nucleofector (Amaxa, Cologne, Germany) using O-06 program. STAT3 expression was detected by anti-STAT3 mouse monoclonal antibody (green in left panel) and anti-6xHis antibody, followed by Alexa 488-conjugated anti-mouse IgG antibody (molecular probe, green in right panel). Red color indicates nuclear counterstaining of propidium iodide. (B) Localization of transfected STAT3 in TY-1. His-tagged STAT3 was detected by anti-6x His antibody in the cytoplasm of B cells (left panel). In the presence of IL-6 (Peprotech, Rocky Hill, NJ, 0.1 ng/ml), transfected STAT3 localizes in the nucleus predominantly (right panel). (C) Cell proliferation assay for STAT3-transfected primary B lymphocytes. Primary B cells were isolated from PBMC. The purity of B cell (CD19+) was >95%. The cells were transfected with STAT3 expression vector expressing STAT3 and CD4 by Nucleofector using U-15 program. Transfection efficiency to primary B cells was around 20%. To increase the proportion of transfected cells, the transfected B cells were separated with CD4 microbeads after 16 h of the transfection (Miltenyi Biotec, Auburn, CA). 48 h after transfection of STAT3 or vector to primary B cells, the proliferation rate was measured with BrdU ELISA (Roche). Raji is an EBV-positive Burkitt lymphoma cell line (untransfected). Numbers in Y-axis indicates absorbance in ELISA. Error bars indicate standard errors of 8 independent experiments.

Acknowledgments

This study was supported by Health and Labor Sciences Research Grants on HIV/AIDS from the Ministry of Health, Labor and Welfare (grants H15-AIDS-005 to H.K.), a Grants-in-Aid for Scientific Research from the Ministry of Education, Culture, Sports, Science and Technology of Japan (grant 19590485 to H.K.), a grant for Research on Health Sciences focusing on Drug Innovation from Japan Health Sciences Foundation (grant SA14831 to H.K.), NIH MO1 RR00096 (to W.N.R.), NIH HL57879 (to M.D.W.), NIH HL 59832 (to M.D.W.), NIH DA022162 (to Y.H.), American Lung Association (to M.D.W.), Japanese Foundation for AIDS Prevention (to Y.H.), Uehara Memorial Foundation (to Y.H.) and the New York University Center for AIDS Research (to Y.H.). The authors declare that they have no competing financial interests.

References

[1] A. Carbone, Emerging pathways in the development of AIDS-related lymphomas, Lancet Oncol. 4 (2003) 22–29.

[2] C. Boshoff, R. Weiss, AIDS-related malignancies, Nat. Rev. Cancer 2 (2002) 373–382.

[3] P.S. Moore, Y. Chang, Kaposi's Sarcoma-Associated Herpesvirus, Lippincott Williams & Wilkins, Philadelphia, 2001.

[4] A. Chadburn, E. Hyjek, S. Mathew, E. Cesarman, J. Said, D.M. Knowles, KSHV-positive solid lymphomas represent an extra-cavitary variant of primary effusion lymphoma, Am. J. Surg. Pathol. 28 (2004) 1401–1416.

[5] S. Hacein-Bey-Abina, C. Von Kalle, M. Schmidt, M.P. McCormack, N. Wulffraat, P. Leboulch, A. Lim, C.S. Osborne, R. Pawliuk, E. Morillon, R. Sorensen, A. Forster, P. Fraser, J.I. Cohen, G. de Saint Basile, I. Alexander, U. Wintergerst, T. Frebourg, A. Aurias, D. Stoppa-Lyonnet, S. Romana, I. Radford-Weiss, F. Gross, F. Valensi, E. Delabesse, E. Macintyre, F. Sigaux, J. Soulier, L.E. Leiva, M. Wissler, C. Prinz, T.H. Rabbitts, F. Le Deist, A. Fischer, M. Cavazzana-Calvo, LMO2-associated clonal T cell proliferation in two patients after gene therapy for SCID-X1, Science 302 (2003) 415–419.

[6] B. Shiramizu, B.G. Herndier, M.S. McGrath, Identification of a common clonal human immunodeficiency virus integration site in human immunodeficiency virus-associated lymphomas, Cancer Res. 54 (1994) 2069–2072.

[7] H. Katano, Y. Sato, T. Kurata, S. Mori, T. Sata, Expression and localization of human herpesvirus 8-encoded proteins in primary effusion lymphoma, Kaposi's sarcoma, and multicentric Castleman's disease, Virology 269 (2000) 335–344.

[8] H. Katano, Y. Sato, T. Kurata, S. Mori, T. Sata, High expression of HHV-8-encoded ORF73 protein in spindle-shaped cells of Kaposi's sarcoma, Am. J. Pathol. 155 (1999) 47–52.

[9] H. Katano, Y. Hoshino, Y. Morishita, T. Nakamura, H. Satoh, A. Iwamoto, B. Herndier, S. Mori, Establishing and characterizing a CD30-positive cell line harboring HHV-8 from a primary effusion lymphoma, J. Med. Virol. 58 (1999) 394–401.

[10] H. Katano, Y. Sato, T. Sata, Expression of p53 and human herpesvirus 8 (HHV-8)-encoded latency-associated nuclear antigen (LANA) with inhibition of apoptosis in HHV-8-associated malignancies, Cancer 92 (2001) 3076–3084.

[11] Y. Asahi-Ozaki, Y. Sato, T. Kanno, T. Sata, H. Katano, Quantitative analysis of Kaposi sarcoma-associated herpesvirus (KSHV) in KSHV-associated diseases, J. Infect. Dis. 193 (2006) 773–782.

[12] T. Koiwa, A. Hamano-Usami, T. Ishida, A. Okayama, K. Yamaguchi, S. Kamihira, T. Watanabe, 5'-long terminal repeat-selective CpG methylation of latent human T-cell leukemia virus type 1 provirus in vitro and in vivo, J. Virol. 76 (2002) 9389–9397.

[13] Y. Hoshino, K. Nakata, S. Hoshino, Y. Honda, D.B. Tse, T. Shioda, W.N. Rom, M. Weiden, Maximal HIV-1 replication in alveolar macrophages during tuberculosis requires both lymphocyte contact and cytokines, J. Exp. Med. 195 (2002) 495–505.

[14] H. Katano, T. Suda, Y. Morishita, K. Yamamoto, Y. Hoshino, K. Nakamura, N. Tachikawa, T. Sata, H. Hamaguchi, A. Iwamoto, S. Mori, Human herpesvirus 8-associated solid lymphomas that occur in AIDS patients take anaplastic large cell morphology, Mod. Pathol. 13 (2000) 77–85.

[15] Y. Hoshino, D.B. Tse, G. Rochford, S. Prabhakar, S. Hoshino, N. Chitkara, K. Kuwabara, E. Ching, B. Raju, J.A. Gold, W. Borkowsky, W.N. Rom, R. Pine, M. Weiden, *Mycobacterium tuberculosis*-induced CXCR4 and chemokine expression leads to preferential X4 HIV-1 replication in human macrophages, J. Immunol. 172 (2004) 6251–6258.

[16] P.O. Brown, B. Bowerman, H.E. Varmus, J.M. Bishop, Retroviral integration: structure of the initial covalent product and its precursor, and a role for the viral IN protein, Proc. Natl. Acad. Sci. USA 86 (1989) 2525–2529.

[17] T. Fujiwara, K. Mizuuchi, Retroviral DNA integration: structure of an integration intermediate, Cell 54 (1988) 497–504.

[18] Y. Hoshino, S. Hoshino, J.A. Gold, B. Raju, S. Prabhakar, R. Pine, W.N. Rom, K. Nakata, M. Weiden, Mechanisms of PMN-mediated induction of HIV-1 replication in macrophages during pulmonary tuberculosis, J. Infect. Dis. (2007) 1303–1310.

[19] D.P. Bednarik, J.A. Cook, P.M. Pitha, Inactivation of the HIV LTR by DNA CpG methylation: evidence for a role in latency, Embo J 9 (1990) 1157–1164.

[20] P.C. Heinrich, I. Behrmann, G. Muller-Newen, F. Schaper, L. Graeve, Interleukin-6-type cytokine signalling through the gp130/Jak/STAT pathway, Biochem. J. 334 (Pt 2) (1998) 297–314.

[21] J.F. Bromberg, M.H. Wrzeszczynska, G. Devgan, Y. Zhao, R.G. Pestell, C. Albanese, J.E. Darnell Jr., Stat3 as an oncogene, Cell 98 (1999) 295–303.

[22] R. Catlett-Falcone, W.S. Dalton, R. Jove, STAT proteins as novel targets for cancer therapy. Signal transducer an activator of transcription, Curr. Opin. Oncol. 11 (1999) 490–496.

[23] T.S. Lin, S. Mahajan, D.A. Frank, STAT signaling in the pathogenesis and treatment of leukemias, Oncogene 19 (2000) 2496–2504.

[24] J. Yang, M. Chatterjee-Kishore, S.M. Staugaitis, H. Nguyen, K. Schlessinger, D.E. Levy, G.R. Stark, Novel roles of unphosphorylated STAT3 in oncogenesis and transcriptional regulation, Cancer Res. 65 (2005) 939–947.

[25] K.L. Nelson, J.A. Rogers, T.L. Bowman, R. Jove, T.E. Smithgall, Activation of STAT3 by the c-Fes protein-tyrosine kinase, J. Biol. Chem. 273 (1998) 7072–7077.

[26] P.G. Pelicci, D.M. Knowles 2nd, Z.A. Arlin, R. Wieczorek, P. Luciw, D. Dina, C. Basilico, R. Dalla-Favera, Multiple monoclonal B cell expansions and c-myc oncogene rearrangements in acquired immune deficiency syndrome-related lymphoproliferative disorders. Implications for lymphomagenesis, J. Exp. Med. 164 (1986) 2049–2060.

[27] R. Merat, A. Amara, C. Lebbe, H. de The, P. Morel, A. Saib, HIV-1 infection of primary effusion lymphoma cell line triggers Kaposi's sarcoma-associated herpesvirus (KSHV) reactivation, Int. J. Cancer 97 (2002) 791–795.

[28] E. Caselli, M. Galvan, F. Santoni, A. Rotola, A. Caruso, E. Cassai, D.D. Luca, Human herpesvirus-8 (Kaposi's sarcoma-associated virus) ORF50 increases in vitro cell susceptibility to human immunodeficiency virus type 1 infection, J. Gen. Virol. 84 (2003) 1123–1131.

[29] A.R. Schroder, P. Shinn, H. Chen, C. Berry, J.R. Ecker, F. Bushman, HIV-1 integration in the human genome favors active genes and local hotspots, Cell 110 (2002) 521–529.

[30] T. Hishima, N. Oyaizu, T. Fujii, N. Tachikawa, A. Ajisawa, M. Negishi, T. Nakamura, A. Iwamoto, Y. Hayashi, D. Matsubara, Y. Sasao, S. Kimura, Y. Kikuchi, K. Teruya, A. Yasuoka, S. Oka, K. Saito, S. Mori, N. Funata, T. Sata, H. Katano, Decrease in Epstein–Barr virus-positive AIDS-related lymphoma in the era of highly active antiretroviral therapy, Microbes Infect. 8 (2006) 1301–1307.

Available online at www.sciencedirect.com
ScienceDirect
Journal of Virological Methods 144 (2007) 79–85
Journal of Virological Methods
www.elsevier.com/locate/jviromet

Rapid detection of human herpesvirus 8 DNA using loop-mediated isothermal amplification

Tomoe Kuhara [a], Tetsushi Yoshikawa [b,*], Masaru Ihira [b], Daisuke Watanabe [a], Yasuhiko Tamada [a], Harutaka Katano [c], Yoshizo Asano [b], Yoshinari Matsumoto [a]

[a] *Department of Dermatology, Aichi Medical University School of Medicine, Aichi, Nagakute, Japan*
[b] *Department of Pediatrics, Fujita Health University School of Medicine, Toyoake, Aichi 4701192, Japan*
[c] *Department of Pathology, National Institute of Infectious Diseases, Shinjuku, Tokyo, Japan*

Received 8 February 2007; received in revised form 27 March 2007; accepted 29 March 2007
Available online 23 May 2007

Abstract

The reliability of a loop-mediated isothermal amplification (LAMP) method for the detection of human herpesvirus 8 (HHV-8) DNA was evaluated. Although LAMP products were produced with the DNA sample extracted from BCP-1 cells, LAMP products were not produced with the DNAs from seven other human herpesviruses. The detection limit of the HHV-8 LAMP method was 100 copies of target sequence/tube. To determine whether the HHV-8 LAMP method could be used to quantify viral DNA, threshold times, which are defined as the time (in s) it takes to reach the threshold turbidity level (0.1), were measured for the amplification of serial dilutions of a DNA plasmid containing the target sequence. The standard curve possessed a correlation coefficient of 0.9428 with a slope of −84.079 and *y*-intercept value of 1936.2. Additionally, an attempt was made to detect viral DNA in 17 specimens collected from Kaposi's sarcomas and two cell lines obtained from primary effusion lymphomas. HHV-8 DNA was detected in 14 of the 17 Kaposi's sarcoma tissue samples and both of the primary effusion lymphoma cell lines. Viral DNA was not detected in HHV-8 LAMP-negative samples using the real-time PCR method.

Keywords: HHV-8; Real-time PCR; LAMP

1. Introduction

Human herpesvirus 8 (HHV-8), which is also called Kaposi's sarcoma-associated herpesvirus, is a member of the subfamily Gammaherpesvirinae, which has been associated with all forms of Kaposi's sarcoma, primary effusion lymphoma, and multicentric Castleman's disease (Boshoff and Chang, 2001; Cesarman et al., 1995; Soulier et al., 1995). In contrast to other human herpesviruses, epidemiological surveys indicate that HHV-8 is not a ubiquitous virus. Areas with a high prevalence of this virus are usually highly endemic for classic or endemic Kaposi's sarcoma. For example, HHV-8 infection is highly endemic in Central, East, and South Africa areas, in which the viral seroprevalence can reach up to 50% in the general population (Dukers and Rezza, 2003). Following the expansion of the human immunodeficiency virus (HIV) type 1 epidemic in Africa, Kaposi's sarcoma is becoming one cancer, which is diagnosed frequently in several African countries (Dedicoat and Newton, 2003). Therefore, an easy and rapid diagnostic procedure for HHV-8 infection would be a valuable tool in these countries. Additionally, it has been reported that HHV-8 can be transmitted during organ transplantations and blood transfusions (De Paoli, 2004) and the risk for the development of Kaposi's sarcoma is high in immunosuppressed organ transplant recipients, monitoring patients for HHV-8 infections is also important in developed countries.

Although a variety of serological assays for the diagnosis of HHV-8 infections have been described, most of them are not sufficiently sensitive or specific. A combination of several assays can be used to obtain adequate degrees of sensitivity and specificity (Chandran et al., 1998; Schatz et al., 2001; Spira et al., 2000). Detection of viral DNA in clinical samples, such as tissues that are thought to be Kaposi's sarcoma or lymphoma cells, is considered to be an appropriate method for determining

* Corresponding author. Tel.: +81 562 939251; fax: +81 562 952216.
E-mail address: tetsushi@fujita-hu.ac.jp (T. Yoshikawa).

0166-0934/$ – see front matter © 2007 Elsevier B.V. All rights reserved.
doi:10.1016/j.jviromet.2007.03.021

whether HHV-8 infection is involved in the pathogenesis of the disease. In addition, because monitoring the viral load can be useful for patient management, real-time PCR is the most valuable method for the diagnosis of HHV-8 infections (Lallemand et al., 2000; Tedeschi et al., 2001; Broccolo et al., 2002a). This method, however, has not yet become a common procedure in hospital laboratories particularly in developing countries, primarily because an expensive thermal cycler is required.

Notomi et al. (2000) described a novel nucleic acid amplification method, termed loop-mediated isothermal amplification (LAMP), which amplifies DNA targets with high specificity, efficiency, and speed. The most significant advantage of LAMP is the ability to amplify specific sequences of DNA under isothermal conditions. Thus, LAMP requires only simple, cost-effective equipment that can be made available easily in hospital laboratories. This is the major advantage for using the method in developing countries, which are highly endemic regions of HHV-8. Because the LAMP protocol exhibits high specificity and high amplification efficiency, this method can be a valuable tool for the rapid diagnosis of infectious diseases (Enosawa et al., 2003; Iwamoto et al., 2003; Kuboki et al., 2003; Ihira et al., 2004; Parida et al., 2004; Yoshikawa et al., 2004; Okamoto et al., 2004; Enomoto et al., 2005; Sugiyama et al., 2005; Kimura et al., 2005; Suzuki et al., 2006) in both commercial and hospital laboratories. The aim of the study was to establish a LAMP-based HHV-8 DNA amplification technique, and its reliability examined for the detection of viral DNA from clinical specimens.

2. Materials and methods

2.1. Study design

HHV-8 DNA extracted from BCP-1 cells was used as a positive control to determine the appropriate conditions for the HHV-8 LAMP protocol, as well as the specificity and baseline sensitivity of this method. DNA from herpes simplex virus (HSV)-1 (KOS strain), HSV-2 (186 strain), varicella-zoster virus (VZV) (Oka-vaccine strain), Epstein-Barr virus (EBV) (peripheral blood mononuclear cells (PBMCs) containing a high copy number of EBV DNA as determined using real-time PCR analysis), human cytomegalovirus (HCMV) (AD-169 strain), human herpesvirus type 6 (HHV-6) A (U1102 strain), HHV-6B (Z29 strain), and human herpesvirus 7 (HHV-7) (RK strain) was used to determine the specificity of the HHV-8 LAMP method. A plasmid containing the HHV-8 target sequence was used to determine the sensitivity of the assay.

In order to determine the reliability of the HHV-8 LAMP method for the detection of viral DNA in clinical samples, two different primary effusion lymphoma cell lines and 17 Kaposi's sarcoma tissue samples (10 of the samples were frozen, whereas the other and seven samples were paraffin-embedded), which

A. Location and name of each target sequence as a primer in HHV-8 ORF26 gene

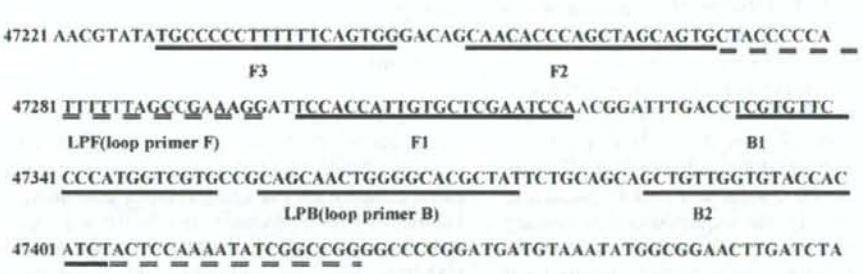

B. Sequence of each primer

Name of primers	Sequence
H8orf26BIP	5'-TCGTGTTCCCCATGGTCGTG AGATGTGGTACACCAACAGC-3' (B1-B2c)
H8orf26FIP	5'-TGGATTCGAGCACAATGGTGGA CAACACCCAGCTAGCAGTG-3' (F1c-F2)
H8orf26B3	5'-CCGGCCGATATTTTGGAGT-3' (B3c)
H8orf26F3	5'-TGCCCCCTTTTTTCAGTGG-3' (F3)
H8orf26LPB	5'-CAGCAACTGGGGCACGCTAT-3' (LPB)
H8orf26LPF	5'-CCTTTCGGCTAAAAAATGGGGGTAG-3' (LPFc)

Fig. 1. (A) Locations and names of the target sequences used as primers for the LAMP of ORF 26 from HHV-8. (B) Names and sequences of the primers for the HHV-8 LAMP method. B2c, sequence complementary to B2; F1c, sequence complementary to F1.

were stored at the Department of Pathology (National Institute of Infectious Diseases, Tokyo, Japan) were used. The results of the HHV-8 LAMP analysis were compared with the results obtained with a previously established HHV-8 real-time PCR assay to assess the reliability of LAMP as a rapid diagnostic tool for detecting HHV-8 infections.

2.2. DNA extraction

For the initial development of the HHV-8 LAMP assay, viral DNA was extracted from BCP-1 cells, PBMCs containing a high copy number of EBV DNA collected from the typical infectious mononucleosis patient caused by primary EBV infection, and HSV-1-, HSV-2-, VZV-, HCMV-, HHV-6A-, HHV-6B-, and HHV-7-infected cells using a QIAamp Blood Mini kit (Qiagen, Chatsworth, CA). This DNA extraction kit was also used to extract DNA from the clinical specimens. After extraction, DNA was eluted in 100 μl of buffer and stored at −20 °C.

2.3. HHV-8 LAMP

The LAMP reaction was conducted according to the descriptions from Notomi et al. (2000) and Nagamine et al. (2002). The LAMP method requires a set of four primers (B3, F3, BIP, and FIP) that recognize a total of six distinct sequences (B1, B2, B3, F1, F2, and F3) in the target DNA. Primers for the HHV-8 LAMP reactions were designed from the sequence of the HHV-8 open reading frame (ORF) 26, which encodes the minor capsid protein, using Primer Explorer V software (FUJITSU, Tokyo, Japan) (Fig. 1). The BIP primer for ORF 26 of HHV-8 (H8orf26BIP) consisted of the sequence of B1 (20 nucleotides; nt) and the sequence complementary to B2 (20 nt). The FIP primer for ORF 26 of HHV-8 (H8orf26FIP) consisted of the sequence complementary to F1 (22 nt) and the sequence of F2 (19 nt). The B3 (H8orf26B3) and F3 (H8orf26F3) primers for ORF 26 of HHV-8 corresponded to the F2-B2 regions. Because it has been demonstrated that additional loop primers increase the amplification efficiency (Nagamine et al., 2002), loop primers for ORF 26 of HHV-8 (H8orf26LPB and H8orf26LPF) were also synthesized. H8orf26LPB consisted of the LPB sequence, and H8orf26LPF consisted of the sequence complementary to LPF. The LAMP reaction was performed with a Loopamp DNA amplification kit (Eiken Chemical, Tochigi, Japan). Each 25-μl reaction mixture contained 2.4 μM H8orf26FIP, 2.4 μM H8orf26BIP, 0.4 μM of each outer primer (H8orf26F3 and H8orf26B3), 1.2 μM of each loop primer (H8orf26LPB and H8orf26LPF), 2× reaction mixture (12.5 μl), *Bst* DNA polymerase (1 μl), and 5 μl of the sample. Reaction mixtures were incubated at 63 °C for 45 min. A LA-200 turbidimeter (Teramecs, Kyoto, Japan) was used to measure turbidity during the LAMP reaction (Mori et al., 2001). The turbidity cutoff value used to distinguish negative samples from positive samples was fixed at 0.1. After turbidity measurements, LAMP products were subjected to electrophoresis on a 1.5% agarose gel. Gels were visualized under UV light after ethidium bromide staining. Great care was taken to avoid contamination between samples; different rooms were used for DNA extraction, LAMP set up, and gel analysis. In addition, pipette tips with filters for aerosol protection were used to minimize contamination.

2.4. Real-time PCR for the detection of HHV-8

Real-time PCR was used to measure the quantity of HHV-8 DNA in each sample. The sequences of the primers and probes have been described by Lallemand et al. (2000). PCR was performed using the TaqMan PCR kit (PE Applied Biosystems, Foster City, CA) according to the manufacturer's protocol. A standard curve for measuring the amount of HHV-8 DNA was constructed using the C_T values obtained from a serially diluted plasmid containing the ORF 73 target sequence. The C_T value from each sample was plotted on a standard curve, allowing copy numbers to be automatically calculated using Sequence Detector v.1.6 software (PE Applied Biosystems).

2.5. Cloning of HHV-8 DNA

In order to determine the sensitivity of the HHV-8 LAMP method, a plasmid containing the target HHV-8 DNA sequence was constructed. First, upstream (H8S1; AACGTATATGCCCCCTTTTT) and downstream (H8S2; TCCGCCATATTTACATCATCC) primers spanning the sequence between the F3 and B3 primers were synthesized. HHV-8 DNA obtained from BCP-1 cells was amplified with these two primers using a conventional PCR. The PCR product was cloned into a pGEM-T vector using pGEM-T Vector System II (Promega, Madison, WI) according to the manufacturer's instructions. The resulting plasmid (pGEMH8S12) was used to make standard dilutions for the evaluation of the lower detection limit of the LAMP protocol.

3. Results

In order to develop an effective assay for the rapid detection of HHV-8 DNA, the specificity of the HHV-8 primers was evaluated. HHV-8 LAMP reactions were performed with DNA extracted from BCP-1 cells, PBMCs containing a high copy number of EBV DNA, and HSV-1-, HSV-2-, VZV-, HCMV-, HHV-6A-, HHV-6B-, and HHV-7-infected cells. Because the LAMP products consisted of several inverted-repeat structures, positive samples result in a number of bands of different sizes following electrophoresis on agarose gels. Although amplified HHV-8 DNA resulted in typical ladder patterns as shown in Fig. 2, no LAMP products were detected in the reactions performed with DNA from other human herpesviruses. The specificity of the primers was tested by using a turbidity assay. The use of HHV-8 specific primers only elevated the turbidity in the HHV-8 DNA-containing samples.

After confirmation of the specificity of the LAMP assay, the sensitivity of this method was determined. Serial dilutions of the pGEMH8S12 plasmid were used to determine the detection limit of the method. Both agarose gel electrophoresis and turbidity assays determined that the detection limit of the HHV-8 LAMP method was 100 copies/tube (Fig. 3). In order to deter-

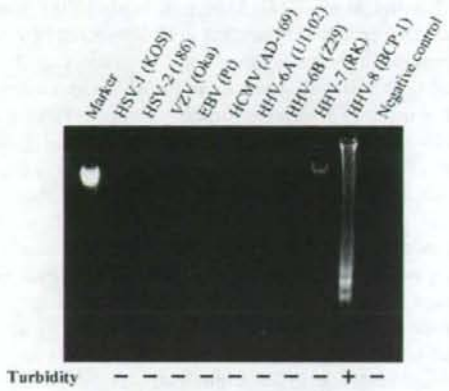

Fig. 2. DNA extracted from cells infected with one of the nine human herpesviruses was amplified using the HHV-8 LAMP protocol to determine the specificity of the method. Marker, 123-base-pair DNA ladder.

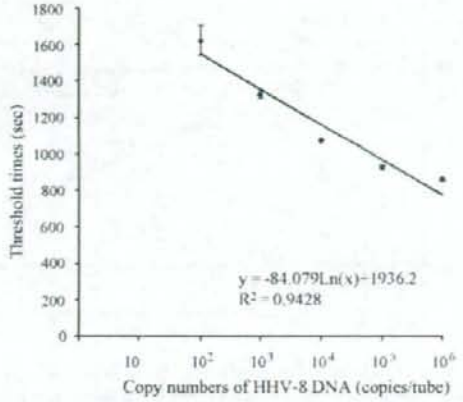

Fig. 4. Correlation between the threshold time (in s) and the copy number of the DNA plasmid (pGEMH8S12) containing the target sequence. Values on the *x*-axis are the threshold times, which are defined as the time it takes to reach the threshold level of turbidity (0.1).

mine whether the HHV-8 LAMP protocol could be used to quantify viral DNA, threshold times, which are defined as the time (in s) it takes to reach the threshold turbidity level (0.1), were measured for the amplification of the serial dilutions of the plasmid DNA. The standard curve possessed a correlation coefficient of 0.9428 with a slope of −84.079 and *y*-intercept value of 1936.2 (Fig. 4) for samples with between 100 and 1,000,000 copies/tube.

After these initial validation studies, the reliability of the HHV-8 LAMP protocol as a rapid method for viral DNA detection from clinical specimens was evaluated. As shown in Table 1, HHV-8 DNA was detected in sample numbers 4–19 using HHV-8 real-time PCR analysis (copy numbers ranging between 138 and 16,594,820 copies/tube). HHV-8 LAMP products were detected using turbidity assays in samples numbers 4–19. Four of the seven DNA samples extracted from the paraffin-embedded Kaposi's sarcoma tissues were determined to be HHV-8 positive using the HHV-8 LAMP assay. In order to determine whether the HHV-8 LAMP could be used to quantify the amount of viral DNA in clinical samples, the correlation between the copy numbers of viral DNA determined using real-time PCR and the threshold times measured with HHV-8 LAMP assay was examined. As shown in Fig. 5, weak association between these two parameters was observed.

4. Discussion

The HHV-8 LAMP method specifically amplified HHV-8 DNA, and did not amplify the DNA from seven other human herpesviruses, including EBV, another member of the *Gammaherpesvirinae* subfamily (Fig. 2). This specificity was confirmed by agarose gel electrophoresis and turbidity assays. The detection limit of the HHV-8 LAMP method was 100 copies/tube, as determined by both agarose gel electrophoresis and turbidity assays. These findings demonstrate that the HHV-8 LAMP method specifically and efficiently amplifies viral DNA. Although the turbidity assay is generally less sensitive than visualizing the ethidium bromide stained products on agarose gels, the sensitivities of these two detection methods were not

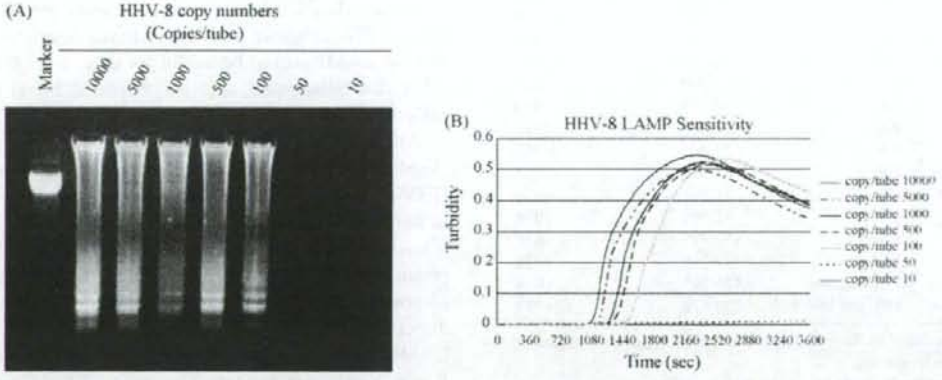

Fig. 3. Serial dilutions of the pGEMH8S12 plasmid were amplified to determine the sensitivity of the assay. Agarose gel electrophoresis (A) and a turbidity assay (B) were both used to determine the sensitivity of the assay. Marker, 123-base-pair DNA ladder.

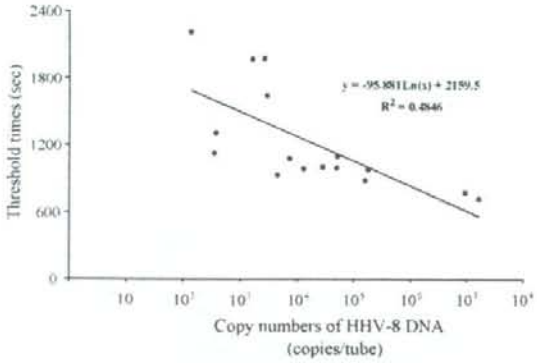

Fig. 5. Correlation between the threshold time (in s) with the viral copy number measured in clinical specimens by real-time PCR. Values on the x-axis are the threshold times, which are defined as the time it takes to reach the threshold level of turbidity (0.1).

significantly different in this study. Compared to agarose gel electrophoresis, turbidity assays allow a reduction in the operation time and reduce contamination risks, and are therefore thought to be an appropriate method for rapid diagnoses in hospital laboratories.

Quantitative analysis of the HHV-8 DNA load using real-time PCR analysis has been demonstrated to be a valuable tool for the management of patients with viral infections. It has been shown that HHV-8 DNA can no longer be detected after the resolution of Kaposi's sarcoma lesions in patients infected with HIV who are being treated with highly active antiretroviral therapies (Burdick et al., 1997; Martinelli et al., 1998). Moreover, the exacerbation of the symptoms in HIV-infected patients with multicentric Castleman's disease has been associated with an increase in the HHV-8 viral load in PBMCs (Grandadam et al., 1997). In order to determine whether or not the HHV-8 LAMP method could be used to quantify the viral DNA load, the threshold times for serial dilutions of a DNA plasmid were measured. Although the standard curve determined using the plasmid dilutions had high correlation efficiency (Fig. 4), the threshold time determined by the HHV-8 LAMP was weakly correlated with the viral copy number measured by HHV-8 real-time PCR analysis in clinical specimens (Fig. 5). One of the reasons for explanation of the low correlation efficiency in the analysis of clinical samples is the difference of the target genes between HHV-8 LAMP and real-time PCR. Additionally, as shown in Fig. 4, it is likely that the reliability of HHV-8 LAMP assay is low for quantitative analysis of samples containing low copies of viral DNA. These results suggest that this method can be used to quantify the high amount of HHV-8 DNA, as has been reported elsewhere (Mori et al., 2001, 2004; Hong et al., 2004; Parida et al., 2004; Suzuki et al., 2006). However, the accuracy of HHV-8 DNA load measured by HHV-8 LAMP method, in particular low amount of viral DNA, appears to be lower than real-time PCR assay. Therefore, if precise quantitation of viral DNA is necessary in the samples containing low copy of viral DNA, real-time PCR would be better than the LAMP method to use at present.

Table 1
Comparison between HHV-8 LAMP and the previously established real-time PCR

No. of samples	Materials	Real-time PCR (copies/tube)	Results of LAMP (s[a])
1	KS[b]	0	−2700<
2	KS[b]	0	−2700<
3	KS[b]	0	−2700<
4	KS	138	+2208
5	KS[b]	353	+1122
6	KS[b]	380	+1302
7	KS	1,640	+1962
8	KS[b]	2,730	+1968
9	KS	2,980	+1638
10	KS	4,570	+930
11	KS	7,560	+1074
12	KS[b]	13,402	+984
13	KS	28,483	+1002
14	KS	51,161	+996
15	KS	52,199	+1098
16	KS	157,878	+876
17	KS	177,798	+978
18	PEL cell line	9,416,765	+774
19	PEL cell line	16,594,820	+720

LAMP: loop-mediated isothermal amplification, KS: Kaposi's sarcoma, PEL: primary effusion lymphoma.

[a] Time required for the turbidity to exceed the cut-off value (0.1).

[b] Paraffin embedded samples.

The prevalence of HHV-8 and the number of patients with acquired immunodeficiency syndrome is low in Japan; accordingly, the frequency of HHV-8-associated diseases, including Kaposi's sarcoma and multicentric Castleman's disease, is also low. Thus, not only the number of clinical samples was limited in this study, but also all materials of clinical samples were restricted within biopsy specimens except for two primary effusion lymphoma cell lines. As it has been demonstrated that HHV-8 DNA loads in peripheral bloods collected from patients with Kaposi's sarcoma were lower than those in the affected tissues (tumoral skin) (Duprez et al., 2005), HHV-8 LAMP method might be less sensitive to detect viral DNA in blood samples. However, as demonstrated in the LAMP method for detection of other viral DNA (Poon et al., 2005), prior-heat denaturation of the template DNA could increase assay sensitivity to detect HHV-8 DNA. Further study is needed to determine whether the HHV-8 LAMP would be useful for detection of viral DNA in other clinical samples such as peripheral blood mononuclear cells and serum.

Although is was observed recently that serum might have slight inhibitory effect in LAMP reactions, a small amount of HHV-6 DNA was detected directly (without DNA extraction) in human serum using the LAMP method (Ihira et al., 2007). It has been demonstrated that the presence of HHV-8 DNA in plasma was associated significantly with the clinical status of Kaposi's sarcoma patients (Broccolo et al., 2002b). Therefore, direct detection of HHV-8 DNA in serum by the HHV-8 LAMP method might be valuable tool for the management of Kaposi's sarcoma patients. Omission of DNA extraction step would be highly advantageous for using the diagnostic method

in developing countries. Large number of sera collected in Kaposi's sarcoma endemic areas should be examined by direct HHV-8 LAMP in a future study.

Acknowledgments

We gratefully acknowledge Eiken Chemical for their contributions to this work. We also thank Mrs. Akiko Yoshikawa and Mrs. Akemi Miki for their technical assistance.

References

Boshoff, C., Chang, Y., 2001. Kaposi's sarcoma-associated herpesvirus: a new DNA tumor virus. Annu. Rev. Med. 52, 453–470.

Broccolo, F., Locatelli, G., Sarmati, L., Piergiovanni, S., Veglia, F., Andreoni, M., Butto, S., Ensoli, B., Lusso, P., Malnati, S., 2002a. Calibrated real-time PCR assay for quantitation of human herpesvirus 8 in biological fluids. J. Clin. Microbiol. 40, 4652–4658.

Broccolo, F., Bossolasco, S., Careddu, A.M., Tambussi, G., Lazzarin, A., Cinque, P., 2002b. Detection of DNA of lymphotropic herpesviruses in plasma of human immunodeficiency virus-infected patients: frequency and clinical significance. Clin. Diagn. Lab. Immunol. 9, 1222–1228.

Burdick, A.E., Carmichael, C., Rady, P.L., Tyring, S.K., Badiavas, E., 1997. Resolution of Kaposi's sarcoma associated with undetectable level of human herpesvirus 8 DNA in a patient with AIDS after protease inhibitor therapy. J. Am. Acad. Dermatol. 37, 648–649.

Cesarman, E., Chang, Y., Moore, P.S., Said, J.W., Knowles, D.M., 1995. Kaposi's sarcoma-associated herpesvirus-like DNA sequences in AIDS-related body-cavity-based lymphomas. N. Engl. J. Med. 332, 1186–1191.

Chandran, B., Smith, M.S., Koelle, D.M., Corey, L., Horvat, R., Goldstein, E., 1998. Reactivations of human sera with human herpesvirus-8 infected BCBL-1 cells and identification of HHV-8 specific proteins and glycoproteins and the encoding cDNAs. Virology 243, 208–217.

Dedicoat, M., Newton, R., 2003. Review of the distribution of Kaposi's sarcoma-associated herpesvirus (KSHV) in Africa in relation to the incidence of Kaposi's sarcoma. Br. J. Cancer 88, 1–3.

De Paoli, P., 2004. Human herpesvirus 8: an update. Microb. Infect. 6, 328–335.

Dukers, N.H., Rezza, G., 2003. Human herpesvirus 8 epidemiology: what we do and do not know. AIDS 17, 1717–1730.

Duprez, R., Kassa-Kelembho, E., Plancoulaine, S., Briere, J., Fossi, M., Kobangue, L., Minsart, P., Huerre, M., Gessain, A., 2005. Human herpesvirus 8 serological markers and viral load in patients with AIDS-associated Kaposi's sarcoma in Central African Republic. J. Clin. Microbiol. 43, 4840–4843.

Enomoto, Y., Yoshikawa, T., Ihira, M., Akimoto, S., Miyake, F., Usui, C., Suga, S., Suzuki, K., Kawana, T., Nishiyama, Y., Asano, Y., 2005. Rapid diagnosis of herpes simplex virus infection by a loop-mediated isothermal amplification method. J. Clin. Microbiol. 43, 951–955.

Enosawa, M., Kageyama, S., Sawaki, K., Watanabe, K., Notomi, T., Onoe, S., Mori, Y., Yokomizo, Y., 2003. Use of loop-mediated isothermal amplification of the IS900 sequence for rapid detection of cultured *Mycobacterium avium* subdp. *Paratuberculosis*. J. Clin. Microbiol. 41, 4359–4365.

Grandadam, M., Dupin, N., Calvez, V., Gorin, I., Blum, L., Kernbaum, S., Sicard, D., Buisson, Y., Agut, H., Escande, J.P., Huraux, J.M., 1997. Exacerbations of clinical symptoms in human immunodeficiency virus type 1-infected patients with multicentric Castleman's disease are associated with a high increase in Kaposi's sarcoma herpesvirus DNA load in peripheral blood mononuclear cells. J. Infect. Dis. 175, 1198–1201.

Hong, T.C., Mai, Q.L., Cuong, D.V., Parida, M., Minekawa, H., Notomi, T., Hasebe, F., Morita, K., 2004. Development and evaluation of a novel loop-mediated isothermal amplification method for rapid detection of severe acute respiratory syndrome coronavirus. J. Clin. Microbiol. 42, 1956–1961.

Ihira, M., Yoshikawa, T., Enomoto, Y., Akimoto, S., Ohashi, M., Suga, S., Nishimura, N., Ozaki, T., Nishiyama, Y., Notomi, T., Ohta, Y., Asano, Y., 2004. Rapid diagnosis of human herpesvirus 6 infection by a novel DNA amplification method, loop-mediated isothermal amplification. J. Clin. Microbiol. 42, 140–145.

Ihira, M., Akimoto, S., Miyake, F., Fujita, A., Sugata, K., Suga, S., Ohashi, M., Nishimura, N., Ozaki, T., Asano, Y., Yoshikawa, T., 2007. Direct detection of human herpesvirus 6 DNA in serum by the loop-mediated isothermal amplification method. J. Clin. Virol. 39, 22–26.

Iwamoto, T., Sonobe, T., Hayashi, K., 2003. Loop-mediated isothermal amplification for direct detection of Mycobacterium tuberculosiscomplex, *M. avium*, and *M. intracellulare* in sputum samples. J. Clin. Microbiol. 41, 2616–2622.

Kimura, H., Ihira, M., Enomoto, Y., Kawada, J., Ito, Y., Morishima, T., Yoshikawa, T., Asano, Y., 2005. Rapid detection of herpes simplex virus DNA in cerebrospinal fluid: comparison between loop-mediated isothermal amplification and real-time PCR. Med. Microbiol. Immunol. (Berl.) 194, 181–185.

Kuboki, N., Inoue, N., Sakurai, T., Di Cello, F., Grab, D.J., Suzuki, H., Sugimoto, C., Igarashi, I., 2003. Loop-mediated isothermal amplification for detection of African trypoanosomes. J. Clin. Microbiol. 41, 5517–5524.

Lallemand, F., Desire, N., Rozenbaum, W., Nicolas, J.C., Marechal, V., 2000. Quantitative analysis of Human herpesvirus 8 viral load using a real-time PCR assay. J. Clin. Microbiol. 38, 1404–1408.

Martinelli, C., Zazzi, M., Ambu, S., Bartolozzi, D., Corsi, P., Leoncini, F., 1998. Complete regression of AIDS-related Kaposi's sarcoma-associated human herpesvirus-8 during therapy with indinavir. AIDS 12, 1717–1719.

Mori, Y., Nagamine, K., Tomita, N., Notomi, T., 2001. Detection of loop-mediated isothermal amplification reaction by turbidity derived from magnesium pyrophosphate formation. Biochem. Biophys. Res. Commun. 289, 150–154.

Mori, Y., Kitao, M., Tomita, N., Notomi, T., 2004. Real-time turbidimetry of LAMP reaction for quantifying template DNA. J. Biochem. Biophys. Meth. 59, 145–157.

Nagamine, K., Hase, T., Notomi, T., 2002. Accelerated reaction by loop-mediated isothermal amplification using loop primers. Mol. Cell Probes 16, 223–229.

Notomi, T., Okayama, H., Masubuchi, H., Yoneyama, T., Watanabe, K., Amino, N., Hzse, T., 2000. Loop mediated isothermal amplification of DNA. Nucleic Acids Res. 28, e63.

Okamoto, S., Yoshikawa, T., Ihira, M., Suzuki, K., Shimokata, K., Nishiyama, Y., Asano, Y., 2004. Rapid detection of varicella-zoster virus infection by a loop-mediated isothermal amplification method. J. Med. Virol. 74, 677–682.

Parida, M., Posadas, G., Inoue, S., Hasebe, F., Morita, K., 2004. Real-time reverse transcription loop-mediated isothermal amplification for rapid detection of West Nile virus. J. Clin. Microbiol. 42, 257–263.

Poon, L.L., Wong, B.W., Chan, K.H., Ng, S.S., Yuen, K.Y., Guan, Y., Peiris, J.S., 2005. Evaluation of real-time reverse transcriptase PCR and real-time loop-mediated amplification assays for severe acute respiratory syndrome coronavirus detection. J. Clin. Microbiol. 43, 3457–3459.

Schatz, O.P., Monini, R., Bugarini, F., Neipel, T.F., Schulz, M., Andreoni, P., Erb, M., Eggers, J., Haas, S., Butto, N., Lukwiya, J.R., Bogner, S., Yaguboglu, J., Sheldon, L., Sarmati, F.D., Goebel, R., Hintermaier, G., Enders, N., Regamey, M., Wernli, M., Sturzl, G., Rezza, Ensoli, R., 2001. Kaposi's sarcoma-associated herpesvirus serology in Europe and Uganda: multicentric study with multiple and novel assays. J. Med. Virol. 65, 123–132.

Soulier, J., Grollet, L., Oksenhendler, E., Cazals-Hatem, D., Babinet, P., d'Agay, M.F., Clauvel, J.P., Raphael, M., Degos, L., Sigaux, F., 1995. Kaposi's sarcoma-associated herpesvirus-like DNA sequences in multicentric Castleman's disease. Blood 86, 1276–1280.

Spira, T.J.L., Lam, S.X., Dollard, Y.X., Meng, C.P., Pau, J.B., Black, D., Burns, B., Cooper, M., Hamid, J., Huong, K., Kite-Powell, P., Pellett, E., 2000. Comparison of serologic assays and PCR for diagnosis of human herpesvirus 8 infection. J. Clin. Microbiol. 38, 2174–2180.

Sugiyama, H., Yoshikawa, T., Ihira, M., Enomoto, Y., Kawana, T., Asano, Y., 2005. Comparison of loop-mediated isothermal amplification, real-time PCR, and virus isolation for the detection of herpes simplex virus in genital lesions. J. Med. Virol. 75, 583–587.

Suzuki, R., Yoshikawa, T., Ihira, M., Enomoto, Y., Inagaki, S., Matsumoto, K., Kato, K., Kudo, K., Kojima, S., Asano, Y., 2006. Development of the loop-mediated isothermal amplification method for rapid detection of cytomegalovirus DNA. J. Virol. Meth. 132, 216–221.

Tedeschi, R., Enbom, M., Bidoli, E., Linde, A., De Paoli, P., Dillner, J., 2001. Viral load of human herpesvirus 8 in peripheral blood of human immunodeficiency virus-infected patients with Kaposi's sarcoma. J. Clin. Microbiol. 39, 4269–4273.

Yoshikawa, T., Ihira, M., Akimoto, S., Usui, C., Miyake, F., Suga, S., Enomoto, Y., Suzuki, R., Nishiyama, Y., Asano, Y., 2004. Rapid diagnosis of human herpesvirus 7 infection by a novel DNA amplification method, Loop-mediated isothermal amplification. J. Clin. Microbiol. 42, 1348–1352.

研究成果の刊行に関する一覧表
平成19年度　慶應義塾大学医学部　熱帯医学・寄生虫学教室　竹内　勤

雑誌

発表者氏名	論文タイトル名	発表誌名	巻号	ページ	出版年
Asao Makioka, Masahiro Kumagai, Seiki Kobayashi, Tsutomu Takeuchi	Differences in protein profiles of the isolates o Entamoeba histolytica and E. dispar by surface-enhanced laser desorpttion ionization time-of–flight mass spectrometry (SELDI-TOF MS) ProteinChip assays	Parasitol Res	102	103-110	2007
H. TACHIBANA ,X.-J. CHENG, S. KOBAYASHI, Y. OKADA, J. ITOH and T. TAKEUCHI	Primary structure, expression and localization of two intermediate subunit lectins of Entamoeba dispar that contain multiple CXXC motifs	Parasitology	134	1989-1999	2007
Sadatomo Tasaka, MD, FCCP; Naoki Hasegawa, MD; Seiki Kobayashi, MD; Wakako Yamada, MD; Tomoyasu Nishimura, MD; Tsutomu Takeuchi, MD; and Akitoshi Ishizaka, MD	Serum Indicators for the Diagnosis of Pneumocystis Pneumonia	CHEST	131	1173-1180	2007
Jun Suzuki, Seiki Kobayashi, Ph.D., Rie Murata, Yoshitoki Yanagawa, D.V.M., and Tsutomu Takeuchi, M.D., Ph.D.	PROFILES OF A PATHOGENIC ENTAMOEBA HISTOLYTICA-LIKE VARIANT WITH VARIATIONS IN THE NUCLEOTIDE SEQUENCE OF THE SMALL SUBUNIT RIBOSOMAL RNA ISOLATED FROM A PRIMATE (DE BRAZZA'S GUENON)	Journal of Zoo and Wildlife Medicine	38	471-474	2007
Taro Fukao, Yoko Fukuda, Kotaro Kiga, Jafar Sharif, Kimihiro Hino, Yutaka Enomoto, Aya Kawamura, Kaito Nakamura, Tsutomu Takeuchi, and Masanobu Tanabe	An Evolutionarily Conserved Mechanism for MicroRNA-223 Expression Revealed by MicroRNA Gene Profiling	Cell	129	617-631	2007

Parasitol Res (2007) 102:103–110
DOI 10.1007/s00436-007-0736-z

ORIGINAL PAPER

Differences in protein profiles of the isolates of *Entamoeba histolytica* and *E. dispar* by surface-enhanced laser desorption ionization time-of-flight mass spectrometry (SELDI-TOF MS) ProteinChip assays

Asao Makioka · Masahiro Kumagai · Seiki Kobayashi · Tsutomu Takeuchi

Received: 4 August 2007 / Accepted: 17 August 2007 / Published online: 11 September 2007

Abstract Surface-enhanced laser desorption ionization time of flight mass spectrometry (SELDI-TOF MS) ProteinChip assays with weak cationic exchange chips were used for protein profiling of different isolates of *Entamoeba histolytica* and *E. dispar*. When SELDI-TOF MS spectra of cell lysates from *E. histolytica* strain HM-1:IMSS were compared with those from four other laboratory strains (200:NIH, HK-9, DKB, and SAW755CR) grown under the same culture conditions, different peak patterns of SELDI-TOF MS were observed among these strains, independent of their zymodeme types. Similarly, five Japanese isolates of *E. histolytica* grown under the same culture conditions revealed different peak patterns among themselves. The SELDI-TOF MS spectra of cell lysates from two isolates of *E. dispar* strain AS16IR and CYNO 09:TPC showed the presence of peaks specific for *E. dispar* isolates and the absence of peaks common to *E. histolytica* isolates. This is not only the first use of SELDI-TOF MS ProteinChip technology for protein profiling of different strains of *Entamoeba* but also the use for parasitic protozoa. The SELDI-TOF MS spectra show a realistic view of proteins with a biological status of *E. histolytica* and *E. dispar* isolates, contributing to show their phenotypic differences of proteins and provide a unique means of distinguishing them.

A. Makioka (✉) · M. Kumagai
Department of Tropical Medicine,
Jikei University School of Medicine,
3-25-8 Nishi-shinbashi, Minato-ku,
Tokyo 105-8461, Japan
e-mail: makioka@jikei.ac.jp

S. Kobayashi · T. Takeuchi
Department of Tropical Medicine and Parasitology,
Keio University School of Medicine,
35 Shinanomachi, Shinjuku-ku,
Tokyo 160-8582, Japan

Introduction

Surface-enhanced laser desorption ionization time-of-flight mass spectrometry (SELDI-TOF MS) ProteinChip assay is a relatively recent technology for exploring proteomes combining chromatography and mass spectrometry (Hutchens and Yip 1993; Issaq et al. 2002). The ProteinChip arrays contain sample spots of 1 or 2 mm diameter, with each chip having a different surface chemistry. These may be chemical (e.g., ionic, hydrophobic, hydrophilic) or biochemical (antibody, receptor, deoxyribonucleic acid [DNA], etc.) and are designed to capture proteins of interest and then analyzed directly on the SELDI-TOF mass spectrometer. The ProteinChip technology has been used for protein profiling and biomarker discovery for diseases such as cancer, neurological disorders, and pathogenic organisms including human African trypanosomiasis (Issaq et al. 2002; Papadopoulos et al. 2004).

Entamoeba histolytica, a protozoan parasite, is responsible for an estimated 40–50 million cases of amebic colitis and liver abscess (WHO/PAHO/UNESCO 1997). There are a large number of isolates of *E. histolytica* that differ in their phenotypes. Although genetic diversity of isolates of *E. histolytica* has been extensively studied, there are few reports on differences in their protein profiles as the phenotype. In this study, we used the SELDI-TOF MS ProteinChip

assays to examine protein profiles of different isolates of *E. histolytica*. We also compared protein profiles of *E. histolytica* with those of nonpathogenic *E. dispar*.

Materials and methods

Five laboratory strains and five Japanese isolates of *E. histolytica* and two isolates of *E. dispar* were used in this study (Table 1). The Japanese isolates of *E. histolytica* were obtained from clinical specimens collected from amebiasis patients in Japan. Axenic in vitro cultures were established and maintained in Diamond's BI-S-33 medium as previously described (Diamond et al. 1978). The two *E. dispar* isolates included one human isolate and one nonhuman primate isolate. The *E. dispar* trophozoites were cultivated axenically in newly designed medium (Kobayashi et al. 2005) with a modification of replacement of gluconic acid with maltose (Kobayashi et al. manuscript in preparation). All cases with intestinal amebiasis or liver abscess were diagnosed by microscopic demonstration of trophozoites or cysts in stool or of trophozoites in liver aspirates, respectively. Zymodeme analysis (Sargeaunt 1988) and polymerase chain reaction analysis (Tachibana et al. 1991; Cheng et al. 1993) of the amoeba isolates were performed to characterize them.

Trophozoites of *E. histolytica* and *E. dispar* in log-phase culture were harvested by centrifugation at 400×*g* for 5 min and washed by centrifugation three times in phosphate-buffered saline and stored in −80°C until use. The pellets of ameba were dissolved in 2% CHAPS (Sigma-Aldrich, St Louis, MO), 5 mM Tris–HCl buffer, pH 8.0 containing proteinase cocktail (Sigma-Aldrich) with 140 μM E-64 by vortexing. After centrifugation at 15,000×*g* for 15 min, the resulting supernatants were used as whole-cell lysates. Protein concentration was determined by Bio-Rad DC protein assay kit (Bio-Rad Laboratories, Hercules, CA) according to the manufacturer's instructions.

One microgram of cell extract diluted into 4 μl of starting buffer was spotted onto each ProteinChip array (originally Ciphergen Biosystems, Fremont, CA; now Bio-Rad Laboratories) with CM10 (weak cation exchanger: Carboxylate). The chips were then incubated at room temperature for 20 min on a shaker. Nonbound proteins and other contaminants were washed from the CM10 ProteinChip arrays with a buffer of 0.1 M ammonium acetate, pH 4.0, three times. Finally, all chips were washed with MilliQ water to remove interfering salts and detergents. After drying, 0.5 μl of saturated energy-absorbing molecule solution (sinapinic acid in acetonitrile [v/v] and trifluoroacetic acid [v/v]) was added twice, and the chips were allowed to air dry. Mass spectrometry analysis was performed by time-of-flight mass spectrometry in a PBS-II mass reader (Ciphergen Biosystems). Spectra were collected using an average 80 nitrogen laser shots. Spectrum analysis was performed using the ProteinChip software version 2.1b (Ciphergen Biosystems). The optimal detection size range was set between 2,000 and 20,000 Da because the system is most effective at profiling low-molecular-weight proteins (i.e., <20 kDa; Issaq et al. 2002). The intensity of each

Table 1 *Entamoeba histolytica* and *E. dispar* isolates used in this study

Isolate	Isolation		Clinical diagnosis	Serology[a] (S)/PCR[b] (P)	Zymodeme[c]
	Location	Year			
E. histolytica					
HM-1:IMSS	Mexico	1967	Dysentery	NA[d]	II
200:NIH	USA	1949	Dysentery	NA	II
HK-9	Korea	1951	Dysentery	NA	II
DKB	UK	1924	Dysentery	NA	II
SAW755CR	UK	1979	Hematophagous trophozoites in feces	NA	XIV
KU43	Japan	2002	Colitis	S +	II
KU46	Japan	2004	Colitis	S +	XXI
KU2	Japan	1988	Colitis	S +	XIX
KU38	Japan	2002	Asymptomatic	S +	II
KU14	Japan	1999	Asymptomatic	S +	XIX
E. dispar					
AS161R	Iran	1997	Abdominal pain	P +	I
CYNO 09.TPC	Philippines	1994	NA	P +	I

[a] Serology was done by enzyme-linked immunosorbent assay, gel diffusion test, and/or indirect fluorescent-antibody test.
[b] PCR analysis using two sets of oligonucleotide primers each (p11 plus p12 and p13 plus p14, respectively) for amplification of the DNAs of *E. histolytica* and *E. dispar* was performed.
[c] Zymodems type I and III are classified as *E. dispar*.
[d] *NA* Not available

of the peaks to be quantified was determined according to externally calibrated standards (Ciphergen Biosystems). According to the manufacturer, the mass accuracy of the spectrometer is 0.1%. The raw intensity data were normalized using the total ion current of m/z between 2,000 and 20,000 for all study sample profiles.

The mean±SE of the intensity of each peak in SELDI-TOF MS spectra from three independent cultures was calculated for all the isolates. The percentages of the number of peaks whose intensities were comparable to between the two isolates were shown as percentage similarity of the peak pattern. From these values, a dendrogram was generated by the unweighted pair-group method with arithmetic mean (UPGMA).

Results

Reproducibility of SELDI-TOF MS spectra tested with *E. histolytica* HM-1:IMSS

SELDI-TOF MS spectra of the whole cell lysates of *E. histolytica* HM-1:IMSS as a standard strain from three independent cultures are shown in Fig. 1. The peak patterns were almost reproducible. The two groups of peaks in which 4.305 and 8.274 kDa as major peaks were detected in a mass range of 3–15 kDa.

Comparison of SELDI-TOF MS spectra between *E. histolytica* HM-1:IMSS and other laboratory strains

SELDI-TOF MS spectra of *E. histolytica* strain HM-1:IMSS were compared with those from four other laboratory strains, 200:NIH, HK-9, DKB, and SAW755CR, grown under the same culture conditions. As shown in Fig. 2, peaks of HM-1:IMSS in the mass range of 3–6 kDa were significantly higher than those of the other four strains. The peaks of 6–8 kDa were low in all the strains. In the mass range of 8–10 kDa, a peak of 8.274 kDa of HM-1:IMSS was significantly higher than those of the other four strains, whereas peaks of 8.568, 8.791, and 9.267 kDa of HM-1:IMSS were lower than those of the other four strains. In addition, the peak of 9.267 kDa revealed different intensities among the other four strains. There were low peaks in the range of 10–15 kDa in all the strains.

Comparison of SELDI-TOF MS spectra between *E. histolytica* HM-1:IMSS and Japanese isolates

SELDI-TOF MS spectra of *E. histolytica* strain HM-1:IMSS were compared with those from five Japanese isolates, KU43, KU46, KU2, KU38, and KU14. As shown in Fig. 3, only KU2 showed lower peaks than HM-1:IMSS in the range of 3–6 kDa. The peak of 5.423 kDa, which was little seen in the laboratory strains except HM-1:IMSS, was detected in the Japanese isolates except KU2. The intensity of the major peak of 4.305 kDa was comparable to or higher than that of HM-1:IMSS in the Japanese isolates except KU2. The Japanese isolates also showed low peaks in the range of 6–8 kDa, although several peaks of KU2 were higher than those of the other four Japanese isolates. In the range of 8–10 kDa, the peak patterns of KU43, KU38, and KU14 were relatively similar to that of HM-1:IMSS, whereas a high peak of 9.267 kDa was observed only in KU2. The peak of 8.568 kDa in KU46 and KU2 was significantly higher than those of HM-1:IMSS and other Japanese isolates. No higher peaks were detected in the range of 10–15 kDa of all the Japanese isolates like the laboratory strains of *E. histolytica*.

Comparison of SELDI-TOF MS spectra between *E. histolytica* HM-1:IMSS and *E. dispar* isolates

SELDI-TOF MS spectra of *E. histolytica* HM-1:IMSS grown in the medium for *E. dispar* were similar to those grown in BI-S-33 medium (Fig. 1; data not shown). When SELDI-TOF MS spectra of HM-1:IMSS were compared with those from *E. dispar* isolates, AS16IR and CYNO 09:TPC, the

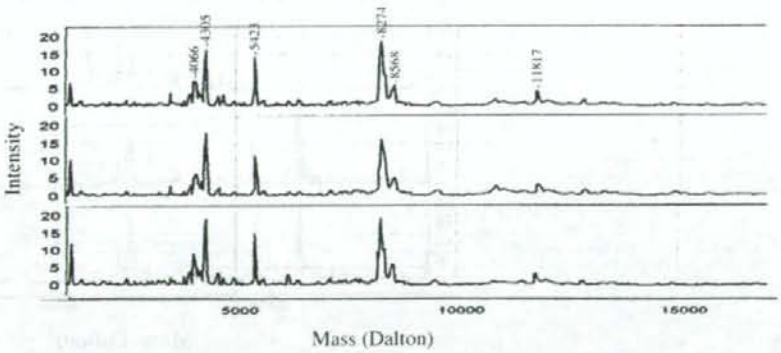

Fig. 1 SELDI-TOF MS spectra of *E. histolytica* strain HM-1:IMSS from three independent cultures. The molecular masses are shown above the peaks